RSC Advances

ROYAL SOCIETY OF CHEMISTRY

www.rsc.org/advances

Table of contents (graphics and text)

This work reveals interesting pathways for water –migration and neutral↔zwitterionic isomerisation in the water complexes of L-proline.

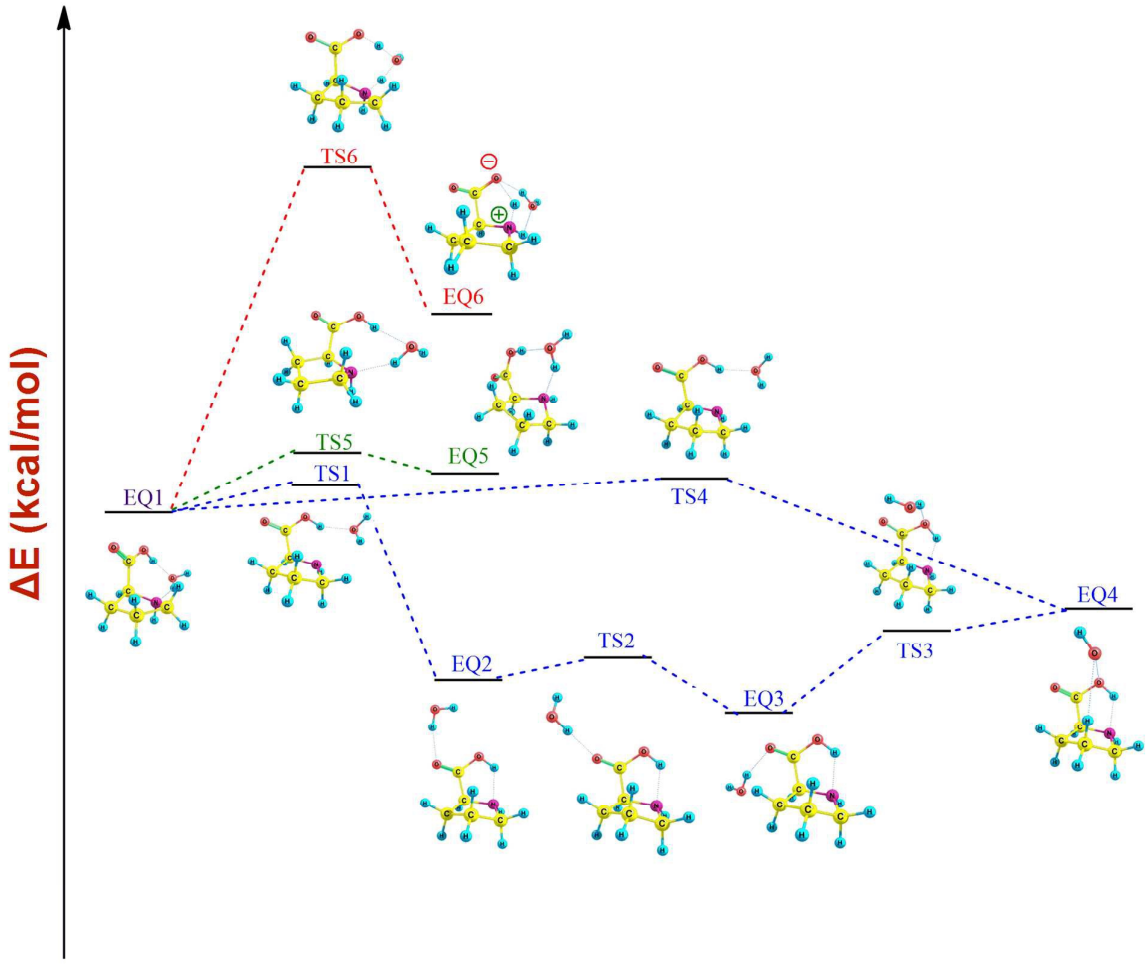

Exploring the Mechanism of Isomerisation and Water-Migration in the Water-Complexes of Amino-acid L-Proline: Electrostatic Potential and Vibrational Analysis

Gurpreet Kaur and Vikas*

Quantum Chemistry Group, Department of Chemistry & Centre of Advanced Studies in Chemistry, Panjab University, Chandigarh- 160014 INDIA.

*Corresponding Author

Email: qlabspu@pu.ac.in, qlabspu@yahoo.com

Phone: +91-172-2534408, +91-9855712099

Abstract

Chemical pathways for the gas-phase isomerisation between the four lowest-lying conformers of amino acid L-proline are proposed using the computations performed through the advanced quantum-mechanical methods like Hatree-Fock, density functional and coupled cluster theories. Besides this, the water-migration pathways in the complexes of L-proline with single-water molecule are presented. The conformers and water-complexes of L-proline are characterized using the spectral analysis involving vibrational frequencies, IR intensities and Raman scattering activities. The effect of electric charge distribution on the mechanism of isomerisation and water-migration is further analysed through the electrostatic potential. The detailed mechanism of the isomerisation in the water complexes, involving zwitterions, has also been unveiled which though is not feasible for the isolated L-proline. Notably, during the isomerisation process of the water-complexes, both positive and negative catalytic effect of the water is encountered. Interesting behaviour in the water-complexes is observed during the analysis of standard Gibbs free-energy change and its temperature-dependence. Besides these, the hydrogen-bonding interaction in the water-complexes of L-proline is also investigated through natural bond orbital analysis. The zwitterionic complexes of L-proline with single-water molecule have also been analysed through the Hirshfeld scheme as well as through widely used population analysis methods.

Keywords: Isomerisation, water migration, proline, zwitterions, catalysis, GRRM.

Introduction

An investigation into the intricate correlations between the reactivity and structure of biomolecules is important because the structure governs biochemical function of molecules and thus, it forms a fundamental basis of most of the biological processes.[1] For example, amino acid proline influences the β-turn in proteins due to the presence of inserted pyrrolidine ring.[2-4] The sequence of such amino acids in a protein determines its conformation and regulates its activity.[5] While contemplating the structure and reactivity of biomolecules, the effect of solvation must be taken into consideration since most of the biochemical reactions occur in a solvent, generally the water.[6-10] The solvation of biomolecules has received considerable attention[6-10] owing to the intermediary conformational structures lying between the isolated and the fully solvated molecules. A perfect example for such a system is the solvation of amino acids which can exist in different conformations depending upon the pH and the extent of the solvation, interestingly, with the intermediates in zwitterionic form.[11-16] The proton-transfer reaction between the carboxylic- and amino-groups involving neutral/zwitterionic isomerisation of amino acid, in the presence of water, has been well studied.[12-16]

The water-solvation of biomolecules can affect the activity, conformation and relative stability of different conformers involved during the solvation. This is also significant from the perspective of catalytic processes, since water can act as an efficient catalyst by stabilizing the biomolecules and/or the corresponding transition states, through the hydrogen bonding.[17-19] For example, Jeon et al.,[13] had studied the isomerization reaction of various conformers of the isolated serine and its water clusters such as neutral serine–$(H_2O)_n$, and zwitterionic serine–$(H_2O)_n$ (n = 1, 2) clusters. These researchers have provided an excellent example for the effect of micro-solvation on the structure and reactivity of biomolecules as their results clearly

demonstrate that the interaction of solvent molecules with the functional group(s) in serine may immensely influence the structure, thermodynamic properties, and reactivity of serine. Besides this, these researchers have also presented the reaction pathways for isomerisation between the neutral and zwitterionic serine in the presence of interacting water molecules, which can crop up either through a concerted double- or triple-proton transfer mechanism depending upon the conformation of serine.

Recently,[19] we had reported water-catalysis in the tautomerisation and geometric isomerisation of thioformic acid while investigating the chemical pathways for water-migration in its water complexes. The molecule of interest in the present study is amino-acid, L-proline, depicted in Figure 1, which is also known as N-alkylated amino acid. It has a distinct cyclic structure with a pyrrolidine ring having an alkyl side group attached to the amino group, resulting in a secondary amine with large basicity. This unique amino acid occurring in natural proteins has been extensively studied due to its ability to act as organocatalyst.[20-23] A definitive *ab initio* structural and energetic study of the conformers of L-proline has been reported by Czinki and Csaszar while exploring the eighteen conformers of the neutral form of L-proline.[24] The solvation-effect of water on the lowest-lying conformers of L-proline has been studied by Lee et al.,[11] who revealed that the water molecule interacting with the proline may have considerable impact on the relative energies of proline. The present work for the first-time maps the pathways for isomerisation in the complexes of L-proline with a single-water molecule while exploring the mechanism of water-migration in these complexes.

This paper is organized as follows: next section describes the computational methodology employed for exploring the reaction pathways in the investigated systems, which is followed by the results and discussion section where a detailed analysis on the mechanism of isomerisation

and water-migration in the proline–water complexes is presented besides analysing the spectral features and electrostatic potentials in the water-complexes of L-proline. Finally, the last section makes a few concluding remarks.

Computational Methodology

All the computations in the present work were performed using a Global Reaction Route Mapping (GRRM)[25-30] method along with Gaussian 03 and Gaussian 09 quantum chemistry software packages.[31,32] Recently, we had successfully employed the GRRM for the exploration of water-catalyzed hydrogen abstraction pathways in thioformic acid,[17] and dithioformic acid,[18] besides revealing the isomerization pathways in radical species like C_6H,[33] C_6N,[34] in molecular anions such as $C_6H_4^{2-}$, $C_6H_3^{3-}$,[35] and also for exploring the stereochemical pathways in serine[36] and 2-aminopropionitrile.[37] In the present work, the initial investigation for the isomerisation pathways in bare L-proline was performed using an anharmonic downward distortion following (ADDF)[25-27] approach of GRRM. The search for the pathways was initially restricted around 20 random geometries, but no relevant pathway could be traced. Then the search was further restricted around previously reported conformers of L-proline (P1, P2, P3 and P4 depicted in Figure 1) by applying a 'FirstOnly' option[28,35,37] of the GRRM at the HF/6-31G level of the Hartree-Fock (HF) theory.

However, the search performed only around P4 was fruitful, which explored six conformers of L-proline, excluding P1 and P2, along with sixteen transition states (which are provided in the supporting information Figure S1). The transition state between conformers P1 and P2 was further explored by guessing and applying the saddle point optimization option in the GRRM. Since, we were interested in the water-complexes of only the four lowest-lying

conformers of L-proline, we had not performed a full-ADDF[28] search through the GRRM, which though is computationally quite expensive but could have provided the water complexes of all the conformers of proline. Initially, the minima and first-order saddle points (the transitions states) were optimized at the HF/6-31G level of theory. All the transition states explored by applying the saddle-point optimization and a double-ended TS search option[28] in the GRRM were then subjected to the intrinsic reaction coordinate (IRC)[38,39] computations through the GRRM program to test the right connectivity between the reactants and products. The geometries obtained were further optimized at the DFT/BHandHLYP/6-311++G(d,p) level of the density functional theory (DFT)[41] theory employing a Becke half and half (BHandHLYP)[40] exchange-correlation functional which uses a 1:1 mixture of DFT with an exact HF exchange energy. The IRC calculations were again performed on the transition state at this level of the theory. Further, the harmonic vibrational frequency analysis was performed for all the structures obtained to testify if the optimized structure located is a minimum or a transition state, and to get the zero-point energy (*ZPE*) correction. All the minima obtained were found to have all frequencies real, while all the interconnecting transition states located had only one imaginary frequency.

The single point energies of all the molecular species were further refined and corrected for the basis set superposition error (BSSE)[42] using the coupled-cluster (CC)[43] theory and counterpoise (CP) method of Boys and Bernardi[44] at the CCSD(T)/6-311++G(d,p)//BHandHLYP/6-311++G(d,p) level of the theory. Through the CP method, the stabilization energy (SE) in the water-complexes of L-proline (AB) is further examined as,

$$\Delta E_{SE(CP)} = E_{AB}(AB) - E_A(AB) - E_B(AB) - [E_A^0(A) - E_A(A)] - [E_B^0(B) - E_B(B)], \quad (1)$$

where $E_X(Y)$ is the energy of the fragment X computed in the basis of Y [with X, Y referring to water-complex of L-proline (AB), or L-proline (A), or H_2O (B)], , E_X^0 is the energy of the

fragment X in its actual geometry within the complex whereas $E_X(X)$ is that of the free fragment in its equilibrium geometry. Besides this, the natural bond-orbital (NBO) analysis[45] was also performed to compute second-order interaction energies in the water-complexes of L-proline.

Result and discussions

Conformers of bare L-proline and their isomerisation pathways

In the present study, the four lowest-lying conformers (P1-P4) of L-proline were considered from a previous study[11] to explore the isomerization pathways for their interconnectivity, and also for their conversion to the possible zwitterionic forms. The latter, to the best of our knowledge, is being investigated for the first time. The explored isomerisation pathways between the four lowest-lying conformers of L-proline are depicted in Figure 1, while their relative energies are reported in supporting information Table S1.

The various conformers of L-proline, depicted in Figure 1, can be analysed on the basis of conformations adopted by pyrrolidine ring.[46] It should be noted that the five-membered pyrrolidine ring conventionally takes up an "envelope"-conformation in order to release the steric and torsional strain. As depicted in Figure 1, the pyrrolidine ring manifests two puckered "envelope" conformations:

(1) an endo ring conformation, where the carbon atom (C3) is puckered towards the carboxylic group, at carbon atom (C2), in a *cis* fashion as in the case of conformers P1 and P3 but with the hydroxyl (OH) of COOH group arranged on the different sides.

(2) an exo ring conformation, where the carbon is puckered away from the carboxylic group at the carbon in a *trans* fashion as in the case of conformers P2 and P4, but with the opposite conformation of the COOH group.

The order of thermodynamic stability of the four conformers of L-proline relative to the lowest-lying isomer P1 at CCSD(T)/6-311++G(d,p)//DFT/BHandHLYP/6-311++G(d,p) level, in kcal/mol, is: P1(0.00) > P2(0.50) > P4(1.38) > P3(1.51) as summarized in Table S1. It was found that conformer P1 can be converted to P2 via transition state TS P1/P2 lying at 1.69 kcal/mol, while P3 can interconvert to P4 via two transition state TS P3/P4(1) and TS P3/P4(2) lying at 1.95 kcal/mol and 2.26 kcal/mol, respectively, at the CCSD(T)/6-311++G(d,p)//DFT/BHandHLYP/6-311++G(d,p) level of theory. This interconversion proceeds through a fluxional behaviour (an up and down movement) of the puckered five-membered ring of L-proline as depicted in Figure 1. However, the direct interconversion between conformers P1 & P3, and between P2 & P4 could not be explored. Interestingly, as depicted in the supporting information Figure S2, the conformers P1 and P2, can also be converted into their zwitterionic forms as explored at the HF/6-31G level of theory, though at the BHandHLYP/6-311++G(d,p) level of the theory, the pathways leading to the zwitterionic forms could not be confirmed. This may be due to complex electron-electron interactions operative in the zwitterions as had also been observed in the previous studies.[15] However, conformers P3 and P4, cannot convert into their respective zwitterionic forms because the hydroxyl (OH) of the carboxylic group, required for the proton-transfer, lies away from the NH group in L-proline.

Further to test the stability of the conformers, the standard Gibbs free-energy change along the dissociation channels (DCs) was analysed at different temperatures, in Table S12, using BHandHLYP/6-311++G(d,p) level of the theory. The present work could trace dissociation channels (DCs), depicted in Figure S1, only for the conformers P3 and P4, whereas the DCs for the conformers P1 and P2 are probably higher-lying in energy. Moreover, the conformers P4 and P3 are found to be stable in the range of room temperature (298K) as indicated by the respective

positive Gibbs free energy change along the DCs, as analysed in Table S12. Besides this, though the DCs for P1 and P2 could not be located but since the conformers P1 and P2 are energetically more stable than conformers P3 and P4, therefore they are too likely to be stable below the room temperature.

Complexes of L-proline with single-water molecule

Though the single-water complexes of four lowest-lying conformers of L-proline had been investigated in a previous study[11] on the interaction of water with proline conformers, however, the detailed mechanism of water-migration and isomerisation in these complexes is being studied here for the first time to the best of our knowledge. The previous study had explored 18 single-water complexes of L-proline, whereas in addition, the present study also reports one new single-water complex, two zwitterionic structures and 22 interconversion transition states. The 19 single-water molecule complexes of proline explored in this work can be organized into four classes as depicted in Figure 2, 3, 5: (I) single-water complexes of conformer P1: Complexes 1a-1e, (II) single-water complexes of conformer P2: Complexes 2a-2e, (III) single-water complexes of conformer P3: Complexes 3a-3e, and (IV) single-water complexes of conformer P4: Complexes 4a-4d. The relative energies of these complexes, with respect to the lowest-lying complex 4b, along with their stabilization energy are provided in supporting information Table S2.

The most relevant single-water complexes with the highest stabilization energy (in kcal/mol) among each class, follows the order as: Complex 1a(11.11)> Complex 2a(10.92)> Complex 3b(10.67)> Complex 4b(10.60), as also analysed in the supporting information Table S2 at the DFT/BHandHLYP/6-311++G(d,p) level of the theory. It should, however, be noted that the relative energy of complexes 1a and 2a, where water is observed to be bridged between the

two functional groups (COOH and NH), with respect to the lowest-lying complex 4b is highest among all the single-water complexes of L-proline. The stabilisation energy estimated using the CP method, through Eq. (1), represents the interaction energy between a conformer of L-proline and a water molecule. Among the complexes of class I and II, respectively, the complexes 1c and 2c are the lowest-lying, where water can be seen interacting with the carbonyl of carboxylic group, from the side of L-proline molecule, opposite to the NH group. It was noticed that the complexes of class I & class II as well as class III & class IV are directly interconvertible, but such direct interconversion between the complexes of class I & class III, class I & class IV, class II & class III , and between class II & class IV, is not observed. For the sake of the brevity, only the direct interconversion is reported in the present work.

Water-migration and isomerisation pathways in the water-complexes of L-proline

The various possible reaction routes involving the water migration and isomerisation in the complexes of L-proline with single-water molecule, among class I and class II complexes, are depicted in Figures 2 and 3, respectively, and in Figure 5 for the complexes of class III and class IV. The neutral-zwitterionic interconversion of conformer P1 involving two- and three-water molecules is further depicted in Figure 4. Besides these, the automeric (self-isomeric) transition states are further displayed in the supporting information Figure S4. It should be noted that a few other reaction routes, as provided in the supporting information Figures S2 and S3, could be explored only at the HF/6-31G level, but at the BHandHLYP/6-311++G(d,p) level of the theory, these could not be ascertained. The reaction overview and relative energy profile along the various pathways are provided in Figures 6 and 7, respectively. The standard Gibbs free-energy change (ΔG) along the relevant pathways is also provided in Table 1 while Table 2 analyses the temperature-dependence of the Gibbs free-energy change relative to the isolated

species, for the dissociation reaction: L-proline–water complex → L-proline + H_2O. The shifts in the scaled[47] vibrational frequencies, along with the corresponding IR intensity and Raman activity, while analysing the spectral features of the conformers and their complexes with single-water molecule, are further provided in Tables S4-S6, whereas the DFT-calculated IR spectra has also been compared with the experimental data, in Table S7-S11 and in Figures 8 and 9, respectively for the conformers P1 and P4, and their complexes with single-water molecule as well as in the presence of water as solvent. The corresponding Raman spectra are provided in Figures 10 and 11, respectively for the conformers P1 and P4. The electrostatic potential (ESP) in the complexes is also analysed, as depicted in Figure 12. Besides these, the second order interaction energies, computed using NBO analysis, are summarized in supporting information Table S3. The zwitterionic complexes are further analyzed using the partial atomic charges summarized in Table 3.

Water-migration and isomerisation in the complexes of class I and II

As evident from Figure 2a, while migrating from complex 1a to 1b, water bridged between the functional groups, moves upward to interact with the carbonyl group of carboxylic acid through transition state complex TS1a/1b, but this involves a conversion barrier of only 0.25 kcal/mol at the CCSD(T)/6-311++G(d,p)//DFT/BHandHLYP/6-311++G(d,p) level of the theory. The water molecule in complex 1b further moves on to the side opposite to the NH group, finally interacting with the C=O group to form complex 1c via transition state complex TS 1b/1c. This migration also proceeds through a very small barrier of 0.06 kcal/mol. Further on, the water molecule moves to interact with the OH group of carboxylic group, on the ring, to form complex 1d via transition state complex TS1c/1d. In the complex 1d, water-migration proceeds again by bridging the water molecule between the functional groups, leading to complex 1a via TS1a/1d

but with a larger barrier height of 3.27 kcal/mol. The latter conversion in the reverse direction is more feasible since the standard Gibbs free-energy change is negative, as analysed in Table 1. All this forms a cycle of water-migration among the class I complexes, as summarised in Figure 6a.

However, in the complexes of class II, only the transition state complex TS 2b/2c could be located, which leads to an interconversion between complexes 2b and 2c. The interconversion between the complexes of class I and class II proceeds mainly through isomerisation in the ring. The activation barrier for the interconversion: Complex 1a↔Complex 2a, is 1.13 kcal/mol which is 0.56 kcal/mol lower than that in the case of P1↔P2 isomerisation between water-free conformers, suggesting a positive water-catalytic effect. However, for the interconversion: Complex 1b↔Complex 2b, the barrier is 1.94 kcal/mol which is 0.25 kcal/mol more than that in the case of interconversion: P1↔P2, indicating a negative catalytic effect of the water as displayed in Figures 1, 2b and supporting information Tables S1-S2. However, interconversion pathways could not be located for the complexes 1e and 2e where the water lie below the ring, and may be interacting with the NH group.

Interestingly, as depicted in Figures 3 and 6a, the complexes 1a and 2a can isomerise to their zwitterionic form by a double proton-transfer through a seven-membered ring transition state complex TS 1a/Z1 and 2a/Z2, respectively, lying at 21.27 and 21.65 kcal/mol. In a previous study,[11] no such zwitterionic complex of L-proline with the single-water molecule was explored but notably, the present study reports two significant pathways involving nuetral↔zwitterionic interconversion in the presence of single-water molecule as found in the complexes 1a and 2a, indicating that the hydrogen bonding from a single-water molecule is significant enough to form stable proline zwitterions. Moreover, the stability of these zwitterions

is evident from the high stabilization energy of 13.49 and 12.24 kcal/mol, observed for complexes Z1 and Z2, respectively, as analysed in the supporting information Table S2.

In order to further investigate upon the probable number of water molecules that can get involved in the transformation of water-complexes of L-Proline to its zwitterionic form, further computations were performed to explore the reaction paths, depicted in Figure 4, involving the complexes of the lowest lying conformer P1 with two and three water molecules. In addition to the single-water molecule zwitterionic complexes Z1 and Z2, it was observed that utmost two water molecules can be directly involved in the triple H-transfer leading to the zwitterionic form, while the third or more water molecules may be indirectly involved through the H-bonding providing further stability to the water-complexes as also observed in a previous study on alanine-water clusters.[12]

Water migration and isomerisation in the complexes of class III and IV

Complex 4b is the lowest-lying complex on the singlet PES of proline-water complexes, as depicted in Figure 7. The activation energy for its conversion to complexes 4a and 4c is 3.26 and 4.27 kcal/mol, respectively, through the transition state complex TS4a/4b and TS4b/4c, respectively, at the CCSD(T)/6-311++G(d,p)//DFT/BHandHLYP/6-311++G(d,p) level of the theory, as depicted in Figure 5a. While migrating from complex 4b to 4a, the water molecule interacting with the carboxylic group, from the top, moves side on to bridge the two functional groups, whereas during migration to 4c, water moves to the side opposite to the NH group, thereby interacting only with the OH of carboxylic group. Further, on moving from complex 4a to 4d, the exchange of proton occurs between hydrogen atom, H10 of water and H8 of NH group of L-proline. The water molecule is observed to be moving to the bottom side interacting only

with the NH group of L-proline via governing transition state complex TS 4a/4d where seven-membered ring formation occurs between the water and two functional groups. However, this exchange interconversion requires the highest activation energy of 69.28 kcal/mol observed in the present study.

Among the complexes of class III, complex 3b is the lowest-lying complex which lays just 0.25 kcal/mol above the complex 4b. The complex 3b can convert to complexes 3a and 3c via transition state complex TS 3a/3b and TS 3a/3b, respectively, lying at 3.33 and 4.4 kcal/mol. Further, in moving from complex 3a to 3e, there is a slight downward movement of the water and change in the orientation of proton on N-atom, which involves a barrier height of 2.89 kcal/mol. Besides these, a proton exchange is observed while moving from complex 3e to 3d via a high-lying transition state complex TS 3e/3d lying at 48.44 kcal/mol in energy. Further, the interconversion between the complexes of class III and IV, can also crop up through the fluxional movement of the five-membered ring of L-proline as depicted in Figure 5b. The activation energy for the interconversions: Complex 3c↔Complex 4c, and Complex 3d↔ Complex 4c, is found to be 0.56 and 6.03 kcal/mol, respectively, via governing transition states vomplex 3c/4c and 3d/4d, which is higher than that in the case of isolated L-proline, exhibiting a negative catalytic effect of the water. It should be noted that the interconversions: Complex 3a↔Complex 4a, and Complex 3b↔Complex 4b, were observed only at the HF/6-31G level of the theory (see supporting information Figure S3), while at the BHandHLYP/6-311++G(d,p) level of the theory, the concerned transition states could not be confirmed, again suggesting electron correlation to be quite significant while exploring the potential energy surfaces of proline-water complexes.[15] Besides the above pathways, two automerisation pathways were also explored, which passes via transition state complexes TS 4a/4a and TS 4b/4b with a barrier of

2.45 and 0.25 kcal/mol, respectively, as depicted in Figure 6b and supporting information Figure S4.

In order to evaluate the covalent component of the hydrogen bonding in the water-complexes of L-proline, the interaction energy between the donor Lewis-type NBOs and the acceptor non-Lewis NBOs is evaluated by 2nd-order perturbation theory through the NBO analysis as presented in the supporting information Table S3. It was observed that the covalent component of O3--H9(O1) hydrogen-bond interaction, in complex 1a, is the strongest among all the complexes because the second-order NBO interaction energy of 17.69 kcal/mol in the $n_{O3(2)} \rightarrow \sigma^*_{O1\text{-}H9}$ orbital-interaction is found to be the highest. Besides this, N1--H10(O3) interaction in complex 2a is observed to be strongest among class I and II complexes where L-proline acts as a donor. Moreover, it was noted that in the complexes 1b and 2b, L-proline acts as only a donor while in complexes 1e and 2e, it act as only an acceptor during the H-bond formation. In case of class III and IV complexes, O3--H9(O2) interaction in complex 3b is observed to be the strongest with second-order NBO interaction energy in the $n_{O3(2)} \rightarrow \sigma^*_{O2\text{-}H9}$ orbital-interaction found to be 14.89 kcal/mol, while the N1--H10(O3) interaction in complex 2a is the strongest when L-proline acts as a donor. In complexes 3d and 4d, L-proline acts as only a donor in the H-bond formation. To further test the strength of the water-complexes with respect to respective dissociation fragments, standard Gibbs free energy change at different temperature was analyzed as provided in Table 2. The complexation of L-proline with the single-water molecule is found to increase with the decrease in the temperature as evident from the increasingly positive free energy change with decrease in the temperature, for the dissociation reaction of the complexes. Interestingly, all the complexes seem to be more stable at low temperature particularly below 100 K.

In order to further analyse the zwitterionic forms of L-Proline, partial atomic charges computed using the Hirshfeld population analysis (HPA)[48] scheme and its recent extension in the form of charge model 5 (CM5)[49] are compared with those obtained from the Mulliken population analysis (MPA)[50] and natural population analysis (NPA),[51] though an iterative version[52] of the Hirshfeld scheme has recently been found to be more useful, for example, in a study on L-asparagine.[53] For the zwitterionic complexes Z1 and Z2 as well as for the conformers P1 and P4 of L-Proline and their most relevant water-complexes, Table 3 compares the partial atomic charges computing using the CM5, HPA, MPA, NPA methods at the BHandHLYP/6-311++G(d,p) level of the theory. It is evident that in the zwitterionic complexes Z1 and Z2, the charge on the nitrogen atom N(1) of NH_3 group is positive (less negative) than that on the oxygen atom O(1) of carboxylic group in L-Proline, thereby, revealing a dipolar nature of the explored zwitterionic complexes of L-proline with a single-water molecule. This is true irrespective of the method used for the analysis of atomic charges in Table 3, though it is quite obvious in the case of HPA.

Vibrational analysis of the conformers and water-complexes of L-Proline

Computed IR and Raman spectra

The aforementioned water-migration and isomerisation pathways explored for the conformers of L-proline and their water complexes were further characterised through the vibrational analysis, in terms of IR frequency and Raman activity, as presented in Figures 8-11 and Table S4, at the DFT/BHandHLYP/6-311++G(d,p) level of the theory. During the isomerisation of the lowest-lying conformer (P1) to conformer P2, the C=O, O–H, and N-H IR stretch, respectively located at the wavenumbers 1802.08, 3444.83, and 3451.86 cm^{-1}, are

observed to be blue shifted (to higher frequency) with respect to the corresponding modes in P1 (located at 1800.44, 3425.64, and 3451.55 cm^{-1}, respectively), whereas the C-O stretch (at 1379.9 cm^{-1}) is red shifted (to lower frequency) with a considerable change in the Raman activity of N-H and O-H stretch. This may be due to strong interaction between the nitrogen atom N(1), and hydrogen atom H(9) of OH group, in conformers P1 and P2, as also evident in Figure 1. However, in the higher-lying conformers P3 and P4, only the O–H IR stretch is blue shifted to 3674.69 and 3674.15 cm^{-1}, respectively, whereas all other IR modes are red-shifted with respect to those in the conformer P1. Moreover, the IR shifts, ranging between 263-249 cm^{-1} are quite considerable for the O-H and C-O stretch, which results mainly due to the intra-molecular hydrogen-bonding interactions as also evident in Figure 1. However, during the isomerisation of conformer P3 to P4, the C=O, C-O, and N-H IR stretch are blue-shifted, respectively, to 1773.46, 1120.91, 3439.49 cm^{-1} with respect to those in the conformer P3 (respectively at 1771.61, 1119.19, and 3433.35 cm^{-1}), except the O-H IR stretch which is red shifted to 3674.15 cm^{-1}, though all the shifts were found with quite a low magnitude.

The complexes of L-proline with single-water molecule were also characterised through the spectral features as presented in Figures 8c-11c and Table S5-S6. In the case of complex 1a to complex 1b isomerisation, a red shift was observed for the O–H stretch in L-proline, from 3454.53 to 3389.13 cm^{-1} while the C=O, C-O, N-H stretching modes in L-proline and symmetric OH stretch in water were observed to be blue shifted (respectively from 1779.6, 1346.84, 3375.22 and 3454.53 cm^{-1} to 1785.69, 1383.47, 3450.22 and 3643.95 cm^{-1}), with a considerable change in the Raman activity for the N-H and O-H vibrational modes. Further following the water-movement as in complex 1c, C=O, O-H, N-H and O-H (water) vibrational modes, except the C-O stretch (which is blue shifted to 1391.64 cm^{-1}), are red shifted, respectively to 1772.04,

3380.14, 3446.59, and 3567.69 cm^{-1}, while the reverse is observed when water-migrates to complex 1d (with shift occurring at wavenumbers 1805.82, 3671.01, 3451.87, 3353.22 and 1382.29 cm^{-1}, respectively), with the latter also accompanied by a red shift for the O–H stretch in water. During the entire water-migration pathway from complex 1a to 1d, only O–H stretch in water is red shifted from 3454.53 cm^{-1} to 3353.22 cm^{-1}, with a small shift in its Raman activity. However, among class I complexes, the IR intensity of N–H stretch at 3424.95 cm^{-1} was observed to be highest in complex 1e, with a significant Raman activity, though a water-migration pathways to this complex could not be located.

During the water-migration among class II complexes, for example, in complex 2b to complex 2c isomerisation, a considerable red and blue shift is observed, respectively, for the O-H stretch in L-proline and water (from 3644.98 and 3411.54 cm^{-1} to 3402.65 and 3560.86 cm^{-1}, respectively). Notably, while migrating from complex 1a to 2a, the O–H IR stretch in water and L-proline is red shifted, from 3454.53 to 3445.67 cm^{-1}, whereas in the case of water-migration form complex 1b to 2b, the C=O and O-H IR stretch are blue shifted, respectively from 1785.69 and 3389.13 cm^{-1} to 1787.48 and 3644.98 cm^{-1}. Besides these, during complex 1d↔complex 2d isomerisation, only the O-H stretch in water is blue shifted (from 3353.22 to 3675.75 cm^{-1}). However, with zwitterion formation, as in complexes Z1 and Z2, the C-O and O-H stretch in L-proline disappear while the C=O and N-H IR stretch are red shifted.

Further, as evident in Table S6, along the water-migration pathways from complex 3a to 3b, C=O, C-O, O-H, N-H and O-H (in water) IR modes are red shifted (respectively from 1749.29, 1143.24, 3670.79, 3456.69, and 3615.68 cm^{-1} to 1730.77, 1127.96, 3394.36, 3432.27, 3606.01 cm^{-1}) with a considerable change in the Raman activity of the O-H stretch in L-proline and water. In moving to complex 3c, while the C=O, O–H stretch (in L-proline and water), are

blue shifted, respectively to 1784.78, 3669.77 and 3680.11 cm^{-1}; the C-O and N-H stretch are red shifted to 1110.62 and 3412.62 cm^{-1}, respectively, with respect to the corresponding modes in complex 3b. In case of Complex 3c↔Complex 3d conversion, considerable frequency shifts were observed for the C-O and symmetric O–H stretch in water, to 1160.06 and 3432.58 cm^{-1}, respectively. On migrating to complex 3e, only the C-O IR stretch is red shifted to 1145.9 cm^{-1} while other modes are blue shifted with respect to those in the complex 3d. On completing a cycle from complex 3e to complex 3a, a blue shift was observed for the N-H and O-H stretch in water (respectively from 3425.78 and 3512.49 cm^{-1} to 3456.69 and 3615.68 cm^{-1}) with a considerable changes in the Raman activity of these modes.

Among class IV complexes of L-proline, during the isomerisation from complex 4a to 4b, while the C-O and N-H IR stretch in L-proline are blue shifted, respectively from 1123.1 and 3426.4 cm^{-1} to 1228.5 and 3439.35 cm^{-1}; the C=O, O-H, in L-proline as well as water, are red shifted from 1751.75, 3669.93 and 3627.76 cm^{-1} to 1732.01, 3398.35 and 3601.15, respectively. In the case of complex 4b to complex 4c isomerisation, only the C-O IR stretch is red shifted to 1228.5 cm^{-1}; whereas when migrating to Complex 4d, only the O-H IR stretch in L-proline is blue shifted from 3667.75 to 3672.89 cm^{-1}. During isomerisation of Complex 3c to Complex 4c, a significant blue shift is observed for the N-H IR stretch from 3412.62 to 3443.37 cm^{-1}; while along complex 3d to complex 4d isomerisation pathway, a considerable red shift is observed for the C-O IR stretch from 1160.06 to 1112.78 cm^{-1}.

Comparison with experimental vibrational spectra and L-proline in water-solvent

The computed IR frequencies and intensities of conformers P1 and P4 in the absence of water and in the presence of single-water molecule as well as in the water-solvent, were further

compared with the experimental data,[54] in Figures 8 and 9, respectively, as done in previous study on L-aspartic acid.[55] The computations for conformers in the presence of water as a solvent were performed using the polarizable continuum model (PCM)[56] at the BHandHLYP/6-311++G(d,p) level of the theory. It should be noted that the conformers of L-proline have 45 normal modes while proline-water complexes have 54 normal modes with *A* symmetry. In the view of the availability of the experimental data,[54] the IR shifts in the two lowest-lying conformers P1 and P4 are discussed. As evident in Figure 8, when compared with the experimental data, a considerable IR frequency shift is clearly evident for the O-H stretch in the case of conformer P1, in the presence as well as in the absence of water, at wavenumbers of 3454.53 and 3425.64 cm^{-1}, respectively. In particular, as evident in Figure 8(b), the shift to 3254.03 cm^{-1}, is minimum when the solvation effects are included while taking the conformer P1 in water-solvent which has also been analysed with experimental data in Table S7. However, as evident in Figure 9, no such significant shift in the O-H stretch is observed for conformer P4, without water as well in the water-solvent, with the corresponding peak located at 3674.15 and 3651.04 cm^{-1}, respectively, except for the single water-molecule complex 4b of conformer P4 for which the O-H stretch is observed at 3398.15 cm^{-1}.

Notably, a large effect of single-water molecule was also observed for complex 1a among the class I complexes of conformer P1. The C=O, C-O and N-H IR modes were observed to be red shifted, respectively to 1779.6, 1346.84, 3375.22 cm^{-1}, except for O–H stretch (which is blue shifted to 3454.53 cm^{-1}), with respect to those in water-free conformer P1 (at 1800.44, 1382.31, 3451.55, 3425.64 cm^{-1}, respectively). Besides this, as analysed in Table S8, for the O–H stretch, a large blue shift to 3671.01 cm^{-1} was observed for complex 1d of conformer P1. For the stretching frequencies of C=O, C-O and N-H, however, when compared to the experimental data

as listed in Table S7, no significant shift is observed both for P1 (with corresponding peaks at 1800.44, 1382.31, and 3451.55 cm^{-1}, respectively), and P4 (with corresponding peaks at 1773.46, 1120.91, and 3439.49 cm^{-1}, respectively). It should be noted that in a previous work reported at the B3LYP/aug-cc-pVDZ level of the theory,[54] the aforementioned IR shifts are observed to be comparatively low in magnitude.

Similarly, Raman scattering activity of conformers P1 and P4 in the absence and presence of water was analysed in Figures 10 and 11, respectively, and also provided in Tables S8-S11. For conformer P1, a considerable Raman shift for the O-H stretch was observed in water-solvent compared to that in the single-water molecule complex 1a, but there no significant shift was observed for the C-H stretch. In the case of conformer P4, there was significant Raman shift when compared with that in the presence of solvent-water, and single-water molecule complex 4b. It should also be noted that the IR and Raman intensities for water complexes 1a, 2a, 3b and 4b were observed to be highest among their respective classes as analysed in Tables S8-S11. Notably, complexes 3b and 4b were observed to be thermodynamically most stable and likely to be more populated.

Electrostatic potential in the water-complexes of L-proline

Finally, in order to assess the effect of electric charge distribution on the mechanism of isomerisation and water-migration, the electrostatic potential (ESP)[57,58] in the water-complexes of L-proline along various pathways (depicted in Figure 7) were further analysed as presented in Figure 12. For the sake of simplicity, only the negative value of the ESP is depicted. The

negative potential is expected to concentrate around the negatively charged centres (the oxygen and nitrogen atoms) as can also be seen in the ESP maps.

As evident from Figure 12(a), an interaction between the electron-rich nitrogen atom (of L-proline) and oxygen-atom (of water molecule) results in an unfavourable ESP as can be seen in complex 4a of conformer P4. However, this can be overcome by water-migration resulting in complexes 4b and 4c, where the water seems to follow the negative ESP so as the negative potential is well-separated (and balanced) on each centre as in the case of complex 4b which is the most stable water-complex observed in the present study as evident in the potential energy profile depicted in Figure 7. In complex 4c, the negative ESP is predominantly concentrated on the nitrogen and carbonyl oxygen of L-proline, which though migrates to the oxygen atom of the hydroxyl group of L-Proline when complex 4c isomerises to the most stable complex 4b. The water-migration can be seen following those pathways along which the electrostatic repulsions are minimized.

Similar trend is observed in the class III complexes (of conformer P3) as evident in Figure 12(b), where also the negative ESP is evenly distributed and well-separated from each other, over the negatively charged centres (the nitrogen atom of L-proline and the oxygen atoms of L-proline and water), as can be seen in complex 3b. The ESP in these complexes correlates with their stability discussed in the previous sections. Complex 3b was found to be nearly as stable as complex 4b. The ESP map in the two differs mainly due to differing conformations of L-proline in P3 and P4, otherwise water-migration follows similar ESP as observed in the case of class IV complexes.

On the contrary, in the water-complex 1a of most stable conformer P1, negative potential was observed to be concentrated only on the oxygen atoms, separately on the L-proline and water, as evident in Figure 12(c). The water-migration is observed to take place such that the negative ESP on the three oxygen atom is augmented as evident from the ESP distribution in complexes 1b and 1c, which in fact is in correlation with the sequential increase in the overall stability from complex 1a to 1c depicted in Figure 7(a). However, during the isomerisation between the neutral and zwitterionic forms, the cumulative negative ESP on the two-oxygen atoms of zwitterionic L-proline tends to exclude that from the oxygen atom of the water molecule since there is already an excess negative charge on the oxygen atoms of the zwitterions, resulting in the water-migration leading to neutral complex 1a, as evident in Figure 12(d). It should, however, be noted that the zwitterionic complexes, Z1 and Z2, are observed with a considerable stabilisation (interaction) energy due to an intra-molecular hydrogen-bonded interaction in L-proline as evident in Figure 3. Form such ESP analysis, more insights into the mechanism of water-migration can thus be obtained.

Conclusion

The present work, for the first time, computationally investigated the gas phase isomerisation and water migration pathways in the single-water molecule complexes of the four lowest-lying conformers of L-proline. A catalytic effect of water is observed during the neutral↔zwitterionic interconversion in L-proline. During the interconversion of L-proline conformers, the hydrogen exchange is found to influence a fluxional behavior of the pyrrolidine ring in proline, mainly through the hydrogen bond formation. Interestingly, this work suggests

that the water migration around L-proline in the gas phase may lead to conversion of neutral L-proline to its zwitterionic form, particularly in the water-complexes of lowest-lying conformers. The standard Gibbs free energy change for these complexes indicates that the complexation of L-proline with water is more feasible than the dissociation, particularly at lower temperatures. However, along the water-migration and isomerisation pathways, the hydrogen exchange is observed to require large activation energy in the water-complexes of high-lying conformers of L-proline. Besides this, significant changes in the spectral behaviour of the conformers and the water-complexes of L-proline were observed during the spectral analysis involving vibrational frequencies, IR intensities and Raman scattering activities. An analysis of the electrostatic potential in the water-complexes further revealed an interesting behaviour of water along the water-migration pathways.

Acknowledgements

One of the authors, GK, thanks University Grants Commission (UGC), India for providing financial support in the form of UGC-SRF(NET) fellowship. The authors are also grateful to Prof. Koichi Ohno for providing GRRM program, and Dr. Neetu Goel and to the Department of Chemistry, Panjab University, Chandigarh for providing other computational software and resources.

Supplementary data

Supplementary data includes Figure S1-S4, Table S1-S11 and input and options applied in some GRRM computations.

References

1. J. O. Eidahl, B. L. Crowe, J. A. North, C. J. McKee, N. Shkriabai, L. Feng, M. Plumb, R. L. Graham, R. J. Gorelick, S. Hess, M. G. Poirier, M. P. Foster, M. Kvaratskhelia, *Nucleic Acids Res.,* 2013, **41**, 3924-36.
2. Y. K. Kang, *J. Phys. Chem. B,* 2004, **108**, 5463-5465.
3. F. A. Momany, R. F. McGuire, A. W. Burgess, H. A. Scheraga, *J. Phys. Chem.* 1975, **79**, 2361-2381.
4. V. S. Ananthanarayanan, S. K. Attah-Poku, P. L. Mukkamala, P. H. Rehse, *Proc. Int. Symp. Biomol. Struct. Interactions*, *Suppl. J. Biosci.,* 1985, **8**, 209–221.
5. C. H. W. Hirs, S. Moore, W. H. Stein, *J. Biol. Chem.,* 1960, **235**, 633-647.
6. E. G. Robertson, J. P. Simons, *Phys. Chem. Chem. Phys*., 2001, **3**, 1-18.
7. T. S. Zwier, *J. Phys. Chem. A*, 2001, **105**, 8827-8839.
8. C. Desfrancois, S. Carles, J. P. Schermann, *Chem. Rev.,* 2000, **100**, 3943-3962.
9. N. J. Kim, H. Kang, G. Jeong, Y. S. Kim, K. T. Lee, S. K. Kim, *J. Phys. Chem. A,* 2001, **104**, 6552-6557.
10. H. J. Neusser, K. Siglow, *Chem. Rev.,* 2000, **100**, 3921-3942.
11. K. M. Lee, S. W. Park, I. S. Jeon, B. R. Lee, D. S. Ahn, S. Lee, *Bull. Korean Chem. Soc.,* 2005, **26**, 909-912.
12. S. W. Park, D. S. Ahn, S. Lee, *Chem. Phys. Lett.,* 2003, **371**, 74–79.
13. I. S. Jeon, D. S. Ahn, S. W. Park, S. Lee, B. Kim, *Int. J. Quant. Chem*., 2005, **101**, 55–66.
14. C. M. Aikens, M. S. Gordon, *J. Am. Chem. Soc.,* 2006, **128**, 12835-12850.
15. S. M. Bachrach, *J. Phys. Chem. A,* 2008**, 112***,* 3722-3730.
16. S. Im, S. W. Jang, S. Lee, Y. Lee, B. Kim, *J. Phys. Chem. A,* 2008**, 112***,* 9767–9770.

17. G. Kaur, Vikas, *J. Phys. Chem. A,* 2014, **118**, 4019-4029.

18. G. Kaur, Vikas, *RSC Adv.,* 2015, **5**, 50989–50998.

19. G. Kaur, Vikas, *Phys. Chem. Chem. Phys.,* 2014, **16**, 24401-24416.

20. A. Berkessel, H. Gröger, *Wiley-VCH: Weinheim*, 2005, 45-165.

21. U. Eder, G. Sauer, R. Wiechert, *Angew. Chem. Int. Ed.* 1971, **10**, 496-497.

22. Z. G Hajos, D. R. Parrish, *J. Org. Chem.* 1974, **39**, 1615-1621.

23. E. R. Jarvo, S. T. Miller, *Tetrahedron* 2002, **58**, 2481-2495.

24. E. Czinki, A. G. Csaszar, *Chem. Eur. J.*, 2003, **9**, 1008-1019.

25. K. Ohno, S.Maeda, *Chem. Phys. Lett.,* 2004, **384,** 277-282.

26. S. Maeda, K. Ohno, *J. Phys. Chem. A* 2005, **109**, 5742-5753.

27. K. Ohno, S. Maeda, *J. Phys. Chem. A,* 2006, **110**, 8933-8941.

28. S. Maeda, Y. Osada, K. Morokuma, K. Ohno, GRRM 11 user manual, 2011 (http://grrm.chem.tohoku.ac.jp/GRRM/).

29. S. Maeda, K. Ohno, K. Morokuma, *Phys. Chem. Chem. Phys.*, 2013, **15**, 3683-3701.

30. S. Maeda, T. Taketsugu, K. Morokuma, K. Ohno, *Bull. Chem. Soc. Jpn.,* 2014, **87**, 1315-1334.

31. M. J. Frisch, G. W. Trucks, H. B. Schlegel, G. E. Scuseria, M. A. Robb, J. R. Cheeseman, Jr., J. A. Montgomery, T. Vreven, K. N. Kudin, J. C. Burant, et al. Gaussian 03, revision E.01; Gaussian,Inc.: Wallingford, CT, 2004.

32. M. J. Frisch, G. W. Trucks, H. B. Schlegel, G. E. Scuseria, M. A. Robb, J. R. Cheeseman, G. Scalmani, V. Barone, B. Mennucci, G. A. Petersson, et al. Gaussian 09; Gaussian, Inc., Wallingford CT, 2013.

33. Vikas, G. Kaur, *J. Chem. Phys*., 2013, **139**, 224311 (Erratum: *J. Chem Phys.,* 2014, **141**, 039901).

34. G. Kaur, Vikas, *J. Comp. Chem.,* 2014, **35,** 1568-1576.

35. P. Sangwan, Vikas, *Theor. Chem. Acc.*, 2015, 134, 99 (DOI:10.1007/s00214-015-1695-6).

36. G. Kaur, Vikas, *Tetrahedron Lett*., 2015, **56**, 142–145.

37. R. Kaur, Vikas, *J. Chem. Phys*., 2015, **142**, 074307.

38. C. Gonzalez, H. B. Schlegel, *J. Chem. Phys.*, 1989, **90**, 2154-2161.

39. C. Gonzalez, H. B. Schlegel, *J. Chem. Phys*., 1990, **94**, 5523-5527.

40. A. D. Becke, *J. Chem. Phys.,* 1993, **98**, 1372-77.

41. R. G. Parr, W. Yang, *Density Functional Theory of Atoms and Molecules* (Oxford University Press, New York, 1989).

42. R. M. Balabin, *J. Chem. Phys.,* 2008, **129**, 164101-164105.

43. K. Raghavachari, G. W. Trucks, J. A. Pople, M. Head-Gordon, *Chem. Phys. Lett*., 1989, **157**, 479-483.

44. S. F. Boys, F. Bernardi, *Mol. Phys.*, 1970, **19**, 553-566.

45. F. Weinhold, *J. Comput. Chem.,* 2012, **33**, 2363–2379.

46. A. M. P. Koskinen, J. Helaja, E. T. T. Kumpulainen, J. Koivisto, H. Mansikkamaki, K. Rissanen, *J. Org. Chem.,* 2005, **70**, 6447-6453.

47. J. P. Merrick, D. Moran, L. Radom, *J. Phys. Chem. A,* 2007, **111**, 11683-11700.

48. F. L. Hirshfeld, *Theor. Chim. Acta*, 1977, **44**, 129-138.

49. A. V. Marenich, S. V. Jerome, C. J. Cramer, D. G. Truhlar, *J. Chem. Theory and Comput.,* 2012, **8**, 527-541.

50. R. S. Mulliken, *J. Chem. Phys.*, 1955, **23**, 1833–1840.

51. A. E. Reed, R. B. Weinstock, F. Weinhold, *J. Chem. Phys.,* 1985, **83**, 735-746.

52. P. Bultinck, C. Van Alsenoy, P. W. Ayers, R. Carbo-Dorca, *J. Chem. Phys.,* 2007, **126**, 144111.

53. G. Zanatta, C. Gottfried, A. M. Silva, E. W. S. Caetano, F. A. M. Sales, V. N. Freire, *J. Chem. Phys.*, 2014, **140**, 124511-14.

54. S. G. Stepanian, I. D. Reva, E. D. Radchenko, L. Adamowicz, *J. Phys. Chem. A*, 2001, **105**, 10664-10672.

55. A. M. Silva, S. N. Costa, B. P. Silva, V. N. Freire, U. L. Fulco, E. L. Albuquerque, E. W. S. Caetano, F. F. Maia, Jr., *Cryst. Growth Des.*, 2013, **13**, 4844−4851.

56. C. J. Cramer, D. G. Truhlar, *Chem. Rev.,* 1999, **99**, 2161-2200.

57. K. S. Sandhya, C. H. Suresh, *Dalton Trans.*, 2014, **43**, 12279–12287.

58. N. R. Dhumal, *Spectrochim. Acta A,* 2011, **79**, 654–660.

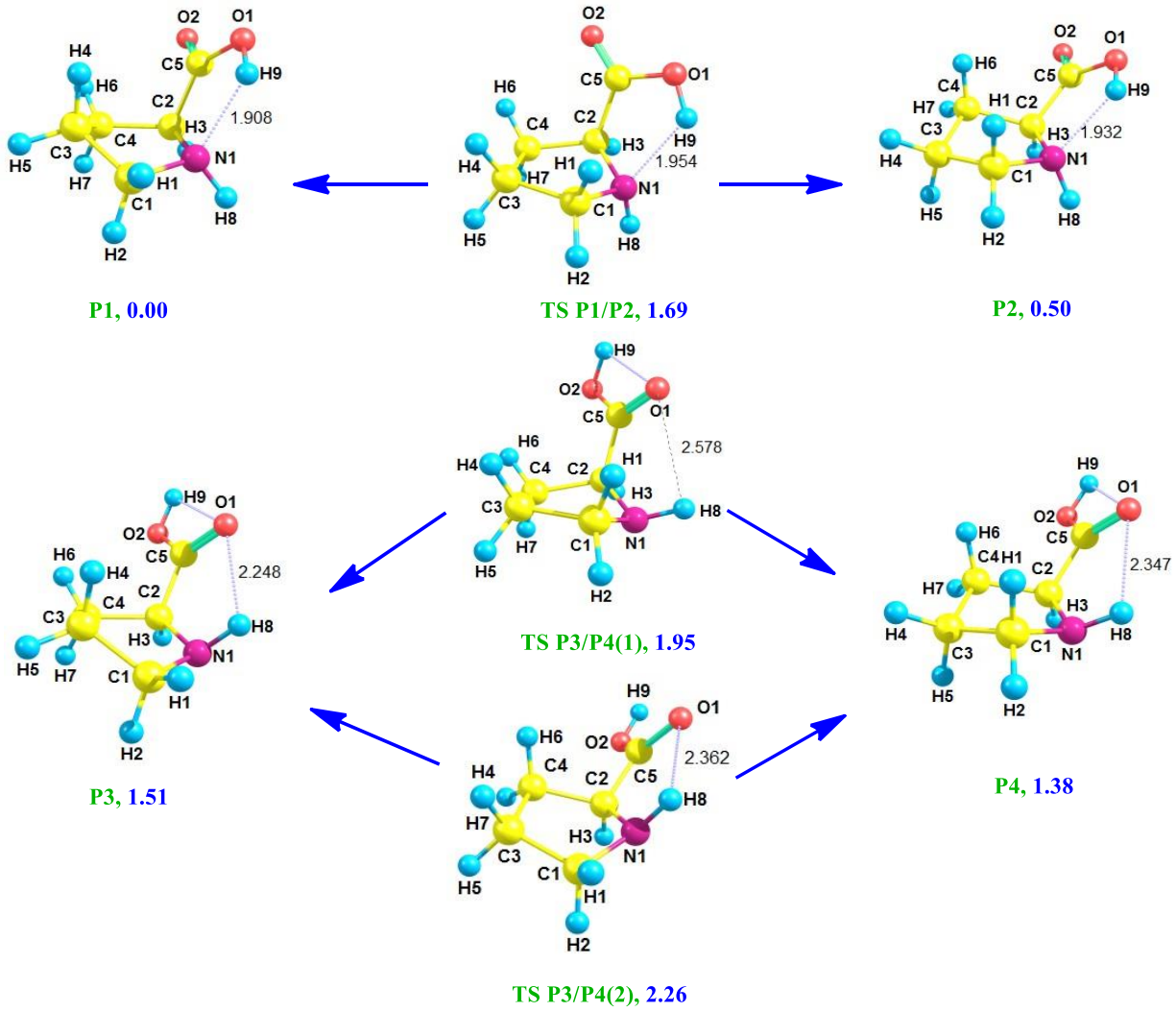

Figure 1. Isomerisation pathways between the four lowest-lying conformers of L-proline (P1-P4). The transition state represented as TS P*n*/P*m* connects the *n*th isomer of proline with *m*th isomer. The geometries (with bond length in Å) are optimized at the DFT/BHandHLYP/6-311++G(d,p) level of theory. The values refers to *ZPE* corrected relative energies (in kcal/mol) with respect to P1 at the CCSD(T)/6-311++G(d,p)// BHandHLYP/6-311++G(d,p) level of the theory.

(a)

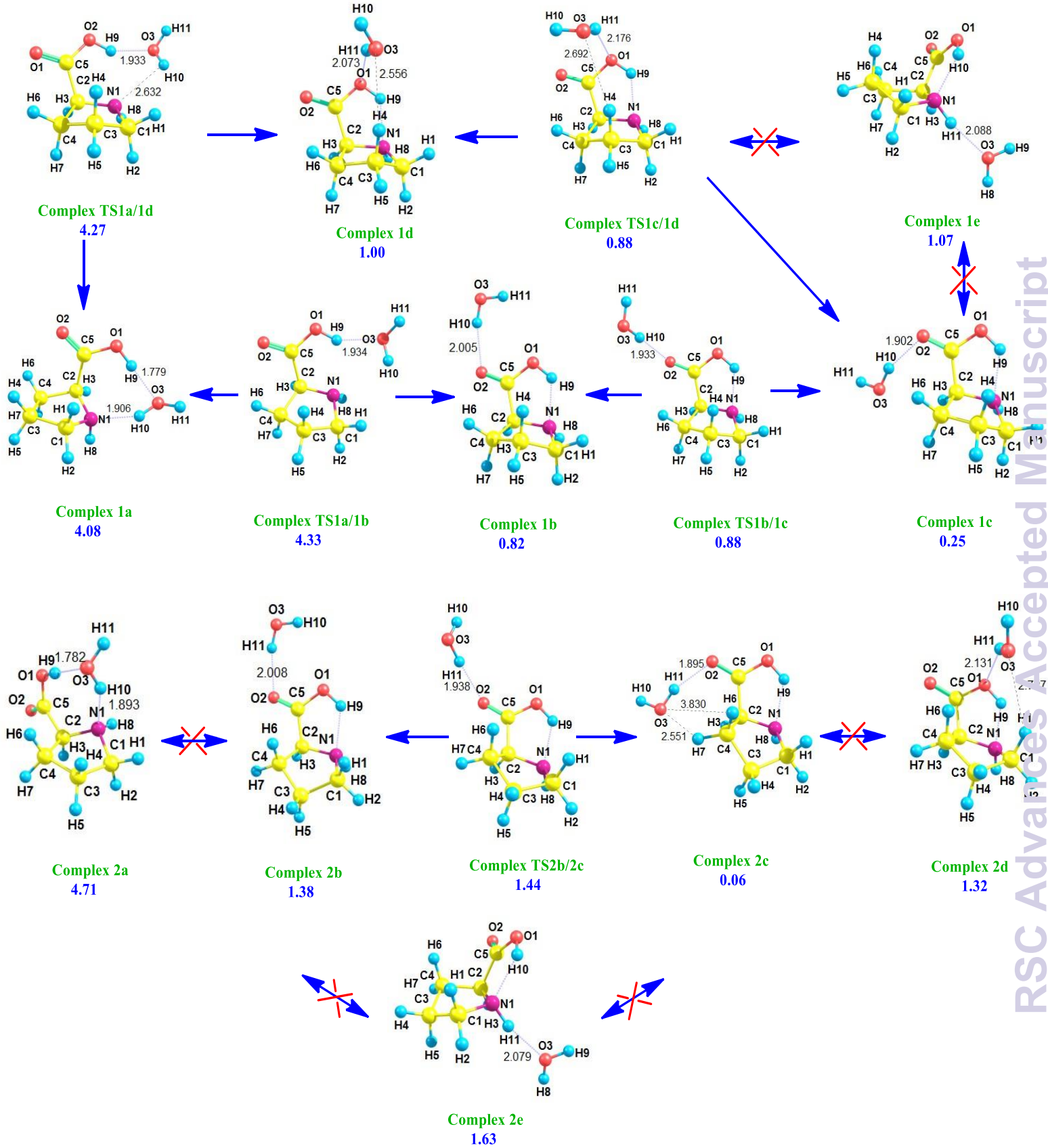

Figure 2 continued…

(b)

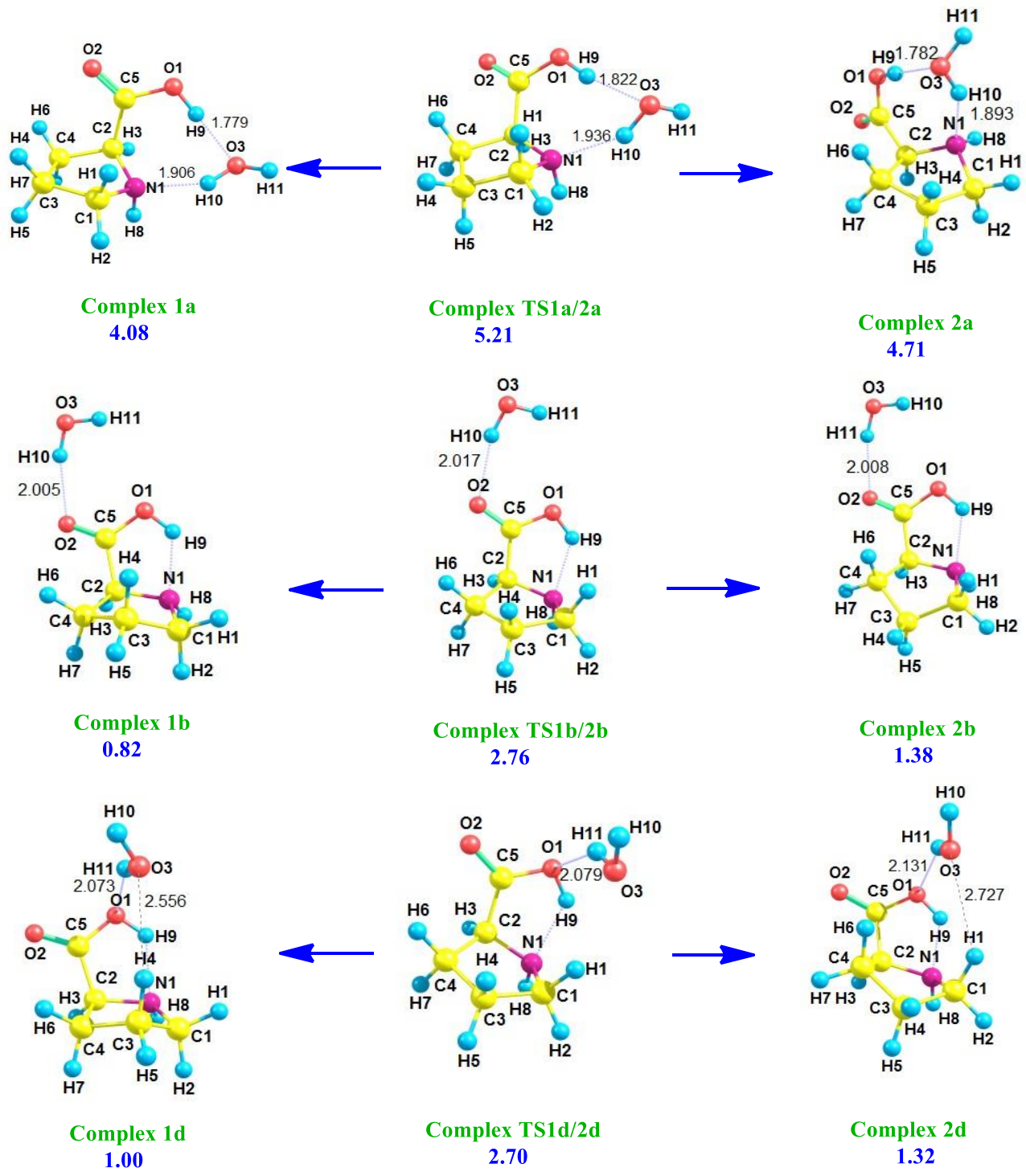

Figure 2. Pathways of: (a) water migration, and (b) isomerisation in the gas phase single-water molecule complexes of L-proline belonging to class I and class II (see the text for details). The geometries (with bond length in Å) are optimized at the DFT/BHandHLYP/6-311++G(d,p) level of theory. The values refer to *ZPE* and BSSE corrected relative energies (in kcal/mol), with respect to Complex 4b of class IV, obtained at the CCSD(T)/6-311++G(d,p)//BHandHLYP/6-311++G(d,p) level of the theory. Complex TS*m*/*n* specifies the transition state interconnecting *n*th proline-water complex with *m*th complex.

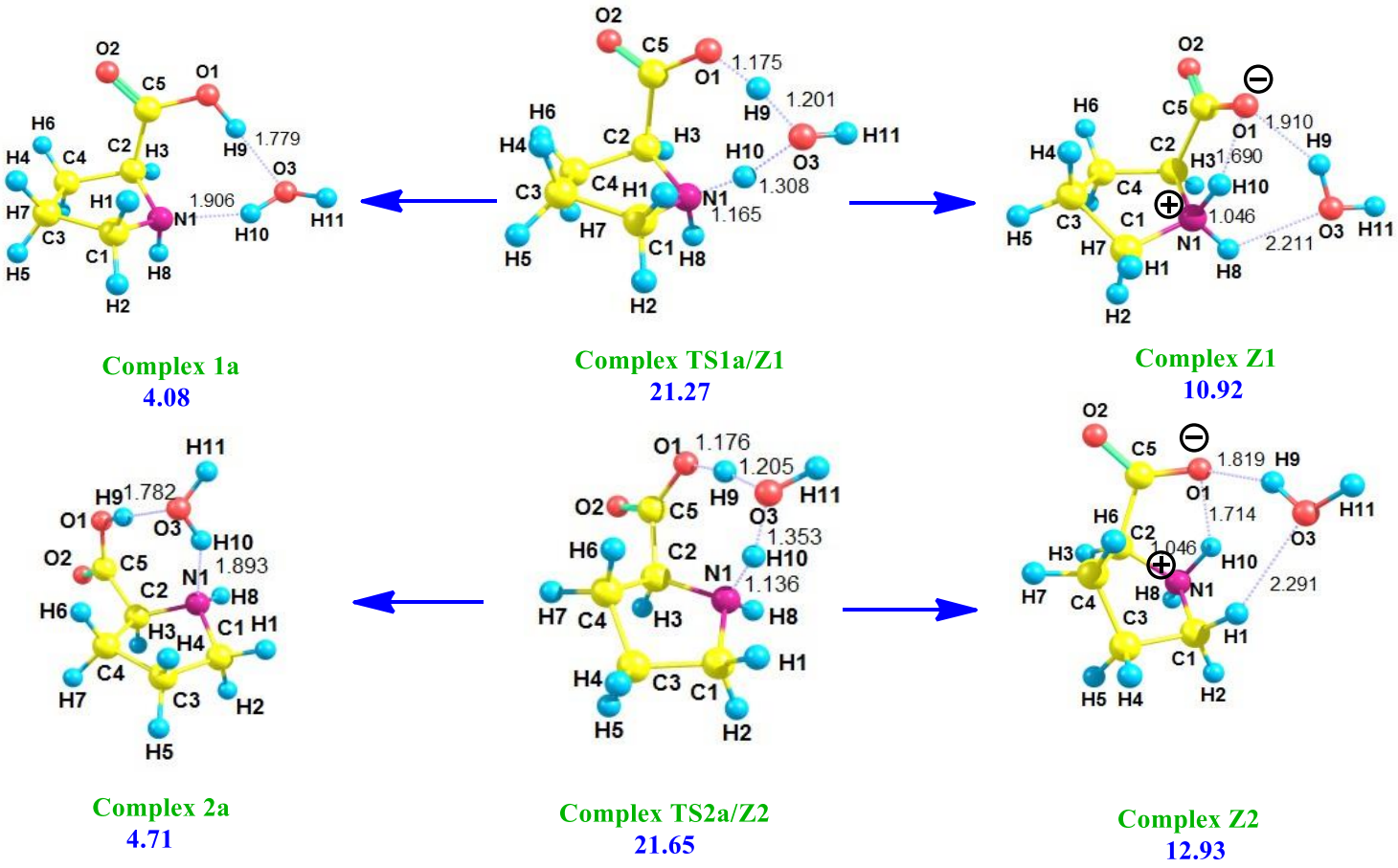

Figure 3. Same as Figure 2, but depicting the water-catalysed interconversion between neutral and zwitterionic forms of L-proline.

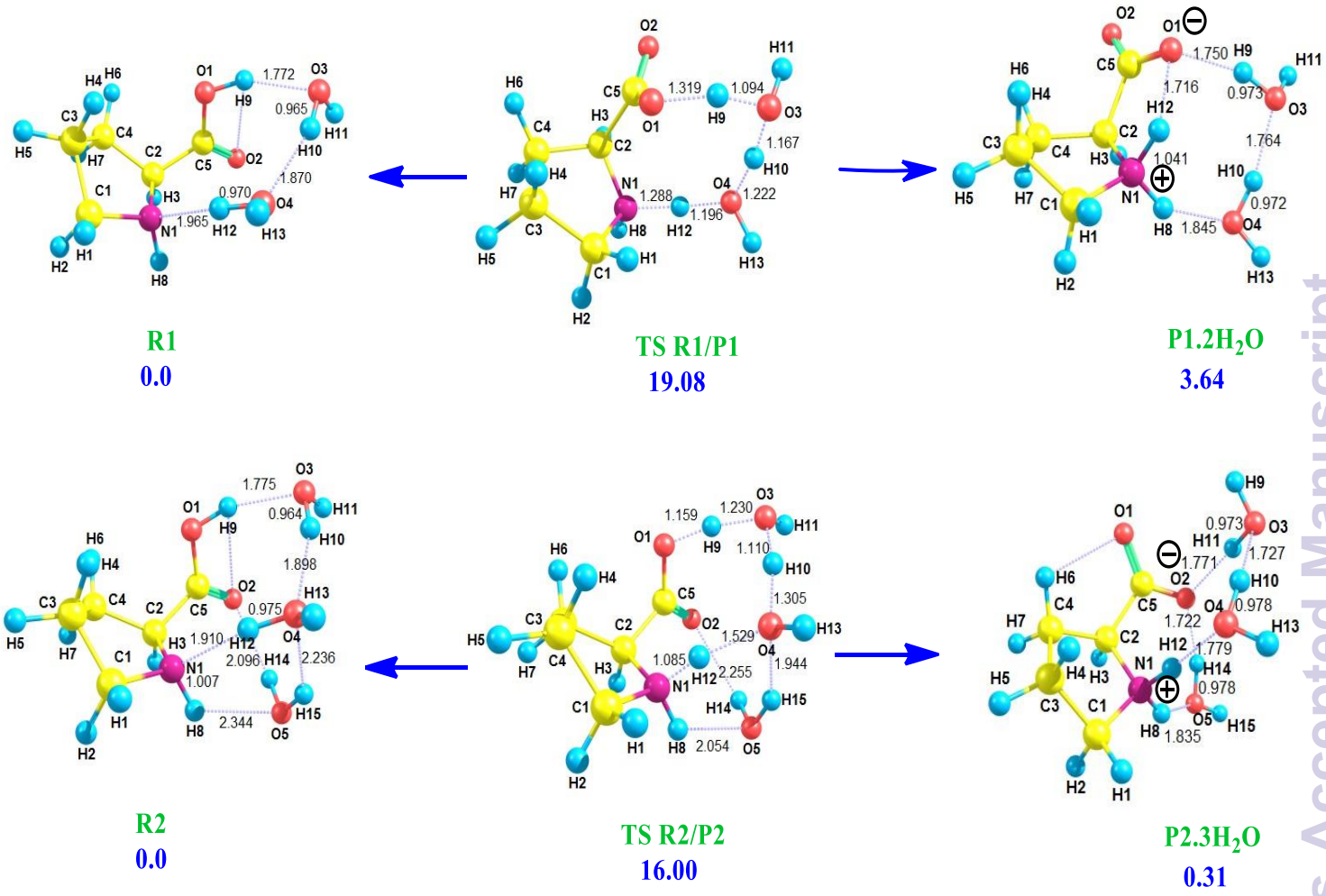

Figure 4. Same as Figure 2, but depicting the two- and three-water molecules catalysed interconversion between the neutral and zwitterionic forms of L-proline. R1 is complex of L-proline conformer P1 with two water molecules and P1.2H_2O is the corresponding zwitterionic complex. R2 is complex of L-proline conformer P1 with three water molecules, and P2.3H_2O is the corresponding zwitterionic complex.

(a)

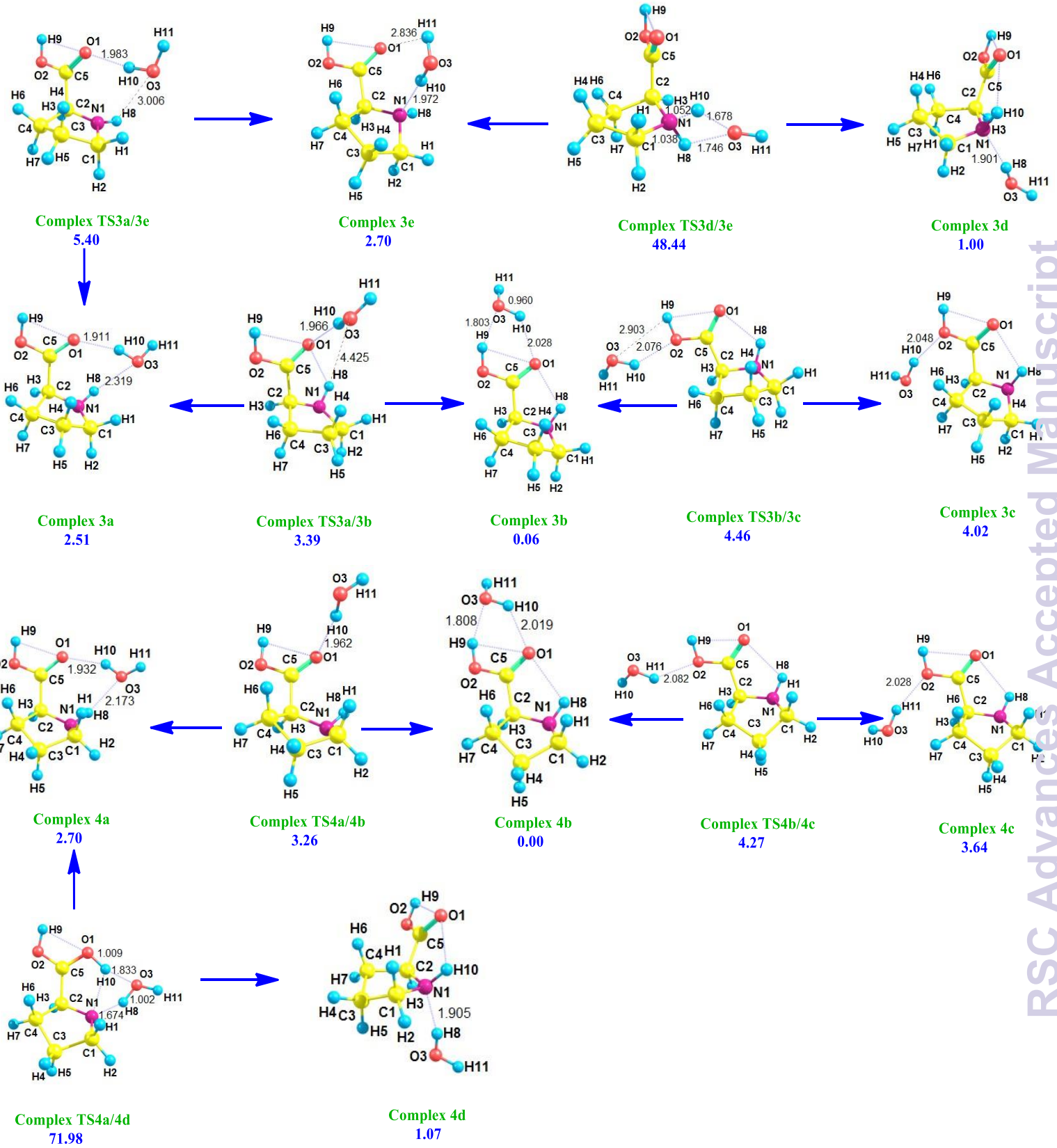

Figure 5 continued….

(b)

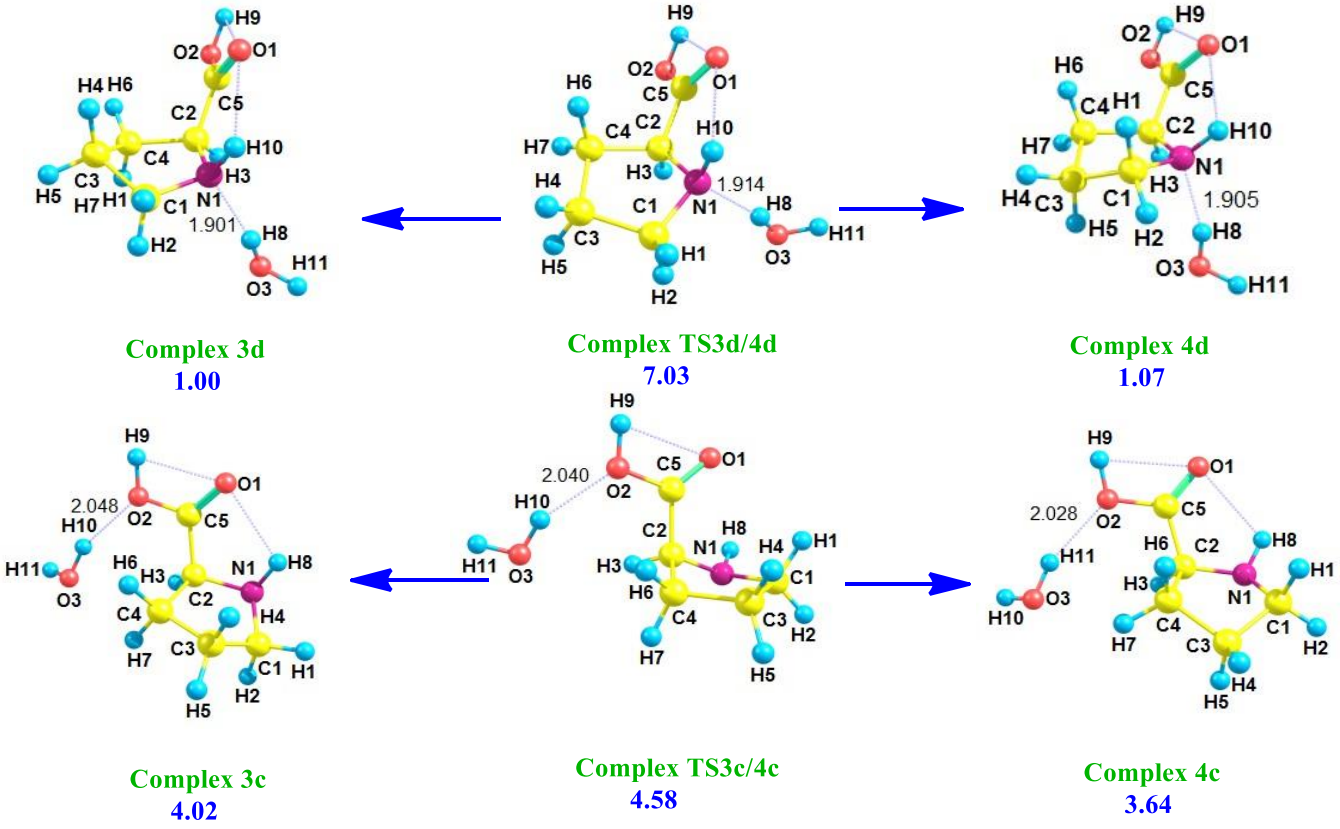

Figure 5. Same as Figure 2a and 2b but for the single-water molecule complexes of L-proline belonging to class III and class IV (see text).

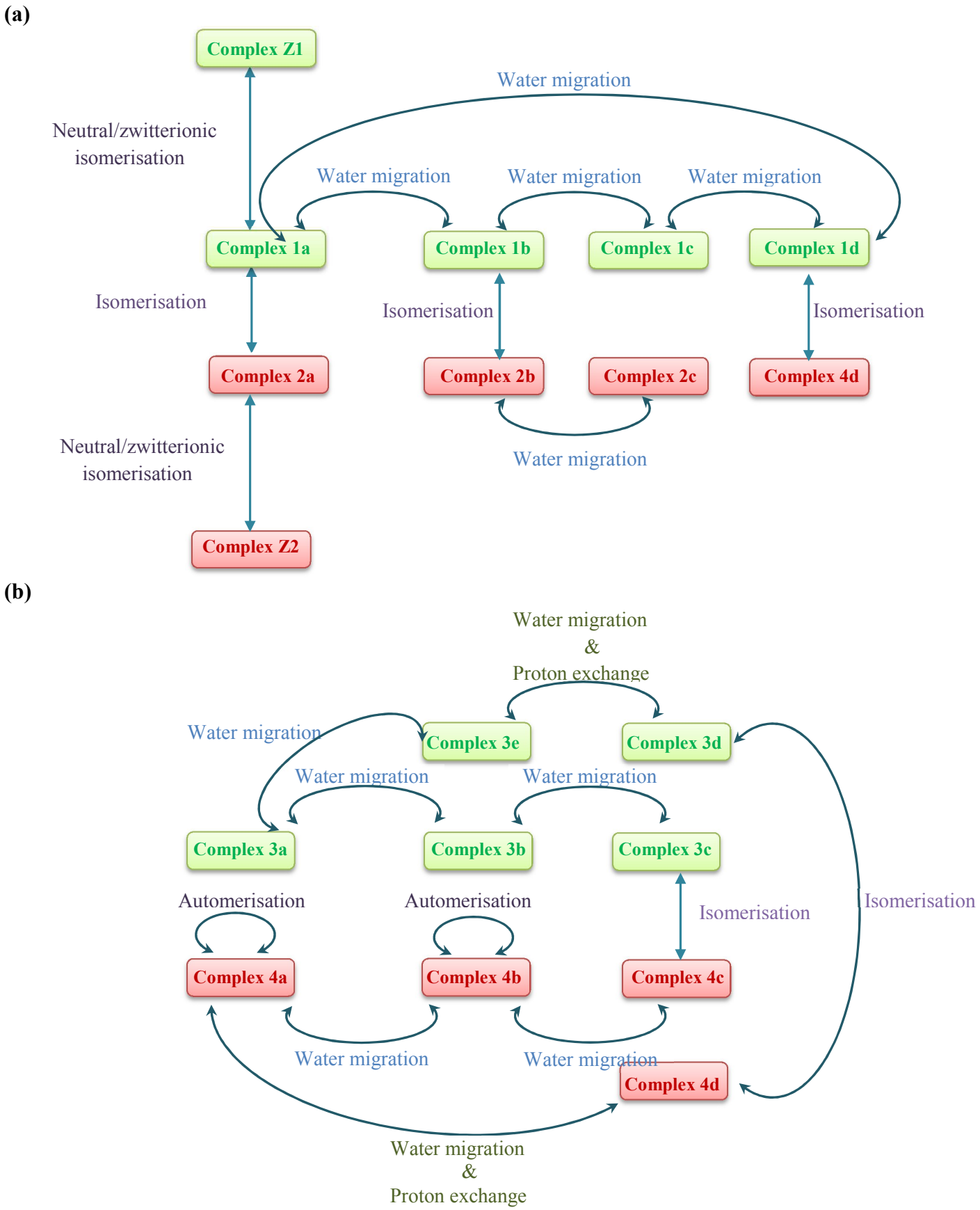

Figure 6. Schematic diagram illustrating different pathways depicted in Figures 2,3,5 involving migration of water molecule and isomerisation in the complexes of L-proline with single-water molecule belonging to: (a) class I and class II, (b) class III and class IV(see text for details).

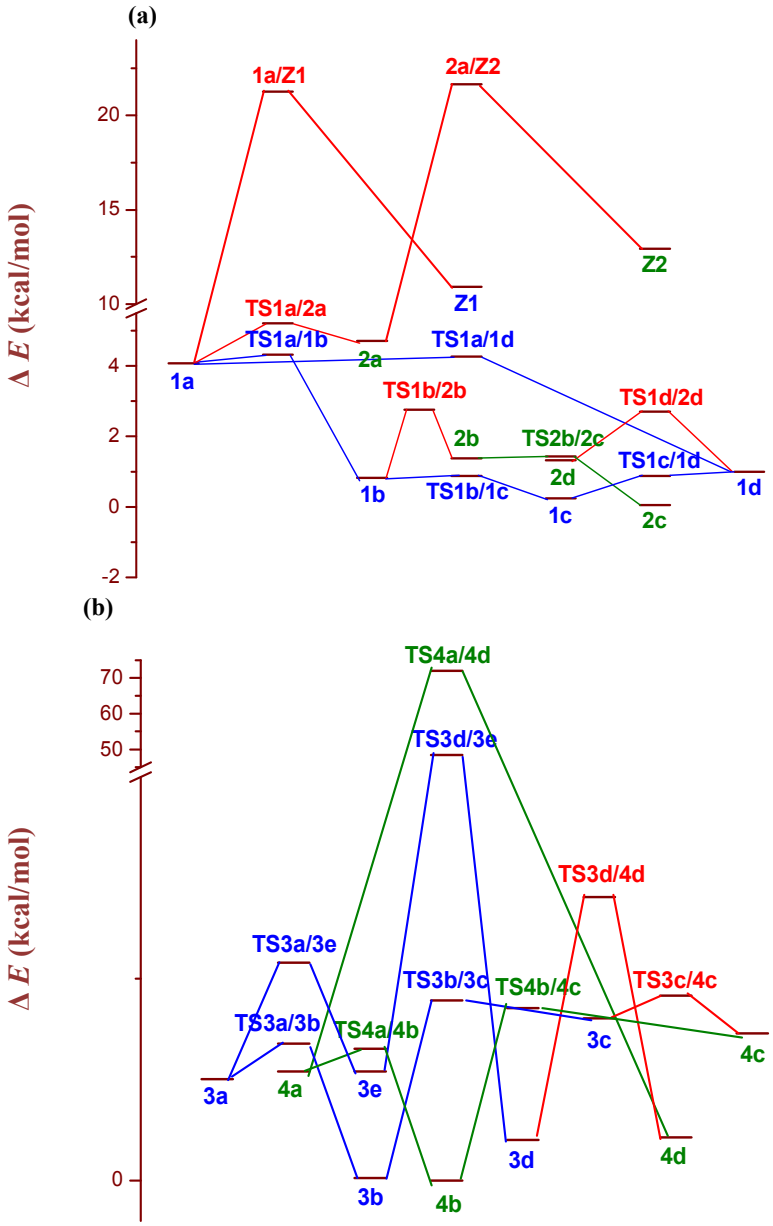

Figure 7. Potential energy profile (in kcal/mol) for the water migration and isomerisation pathways in L-proline-water complexes belonging to (a) class I and class II, (b): class III and class IV, at *ZPE* and BSSE corrected CCSD(T)/6-311++(d,p)//BHandHLYP/6-311++G(d,p) level of the theory. The relative energy (ΔE) depicted is with respect to Complex 4b. Complex TS*m*/*n* specifies the transition state interconnecting *n*th TFA-water complex with *m*th complex.

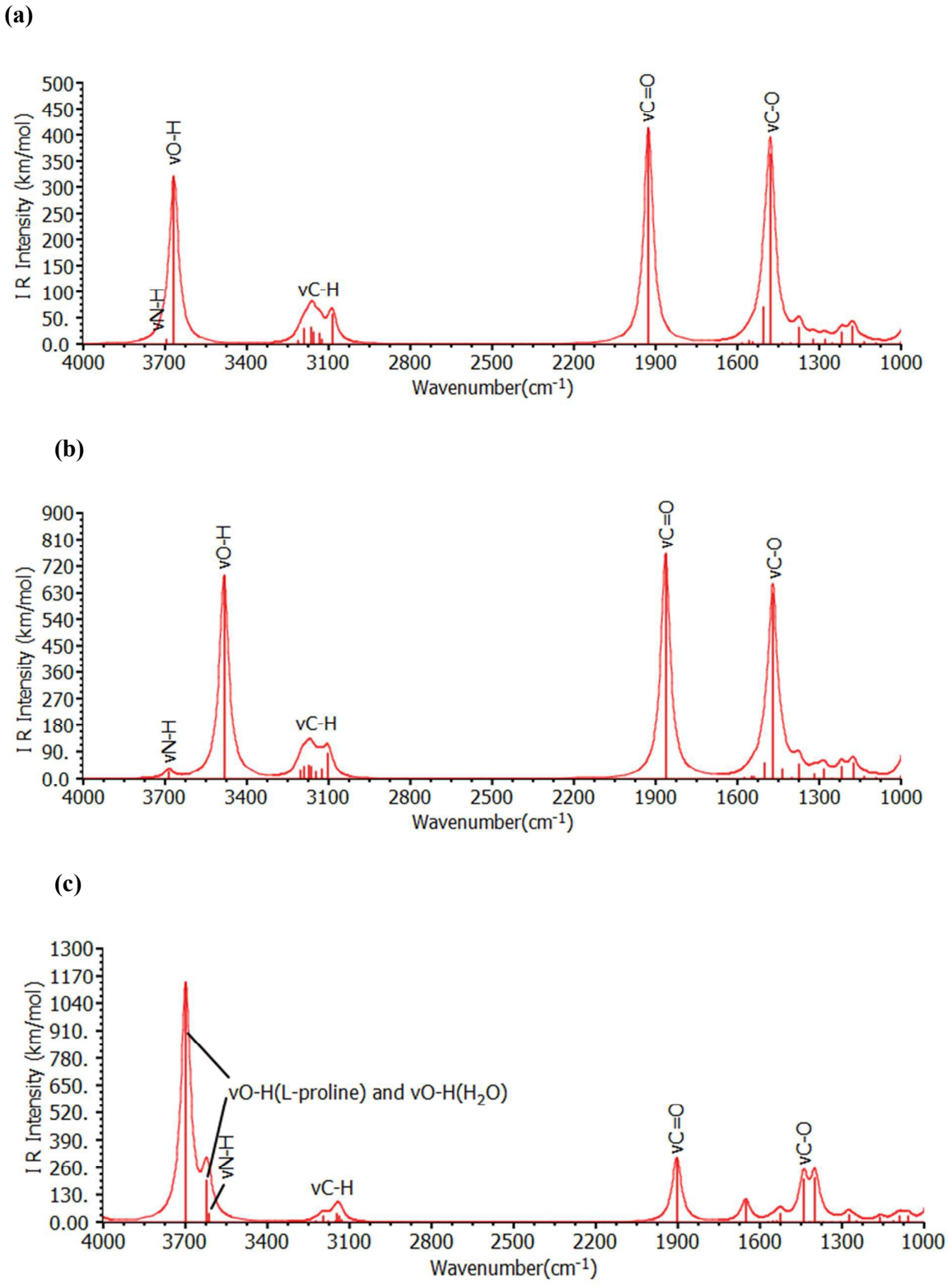

Figure 8. Computed IR spectra of the conformer P1 of L-proline: (a) isolated (gas-phase) P1, (b) P1 in water-solvent, (c) single-water molecule Complex 1a of conformer P1. The vibrational frequencies (wavenumbers), computed at the BHandHLYP/6-311++G(d,p) level of the theory, are unscaled. The vertical lines, under the peaks, specify the location of the normal modes.

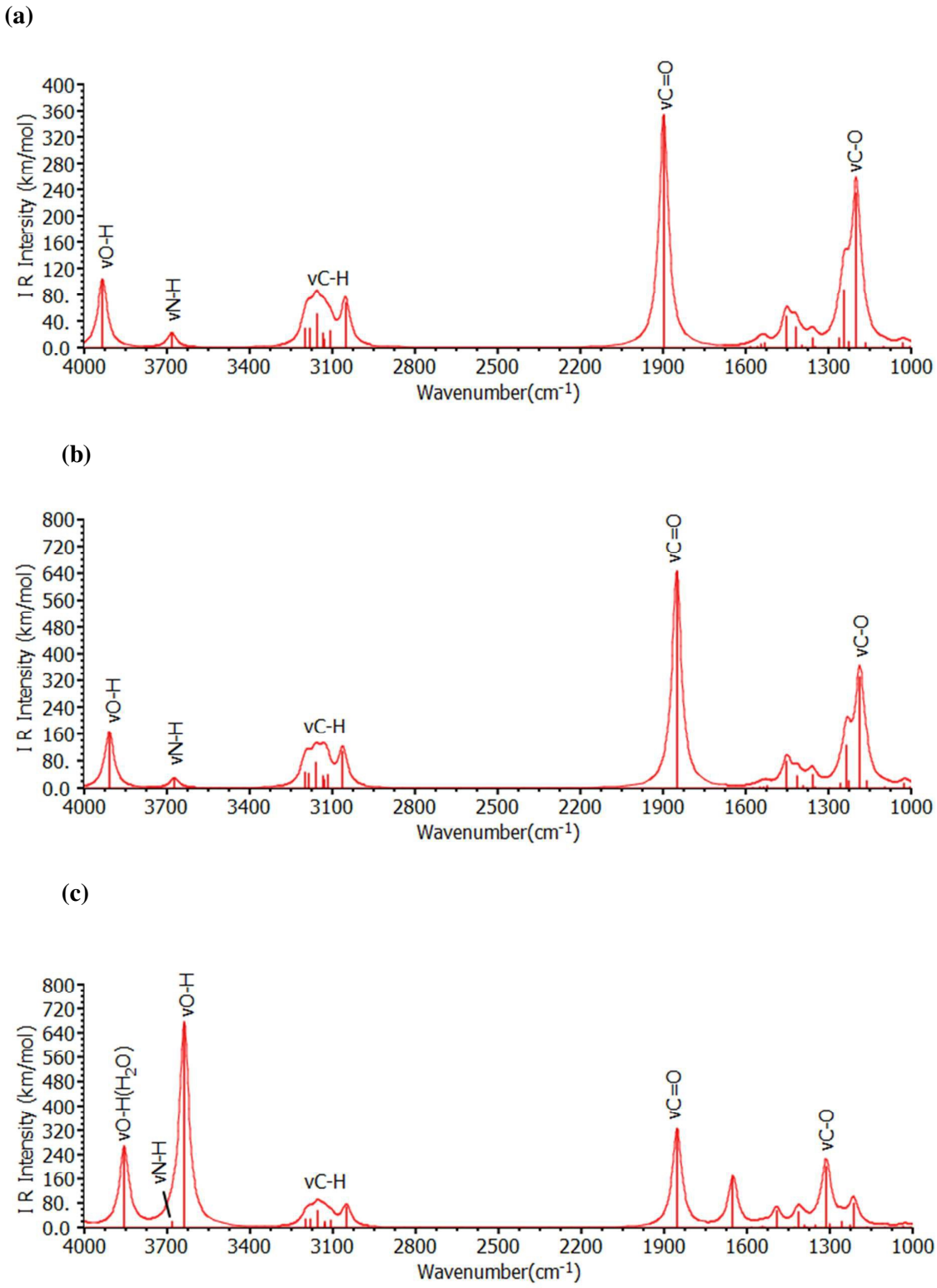

Figure 9. Same as Figure 8, but for the IR spectra of conformer P4 of L-proline and its single-water molecule Complex 4b.

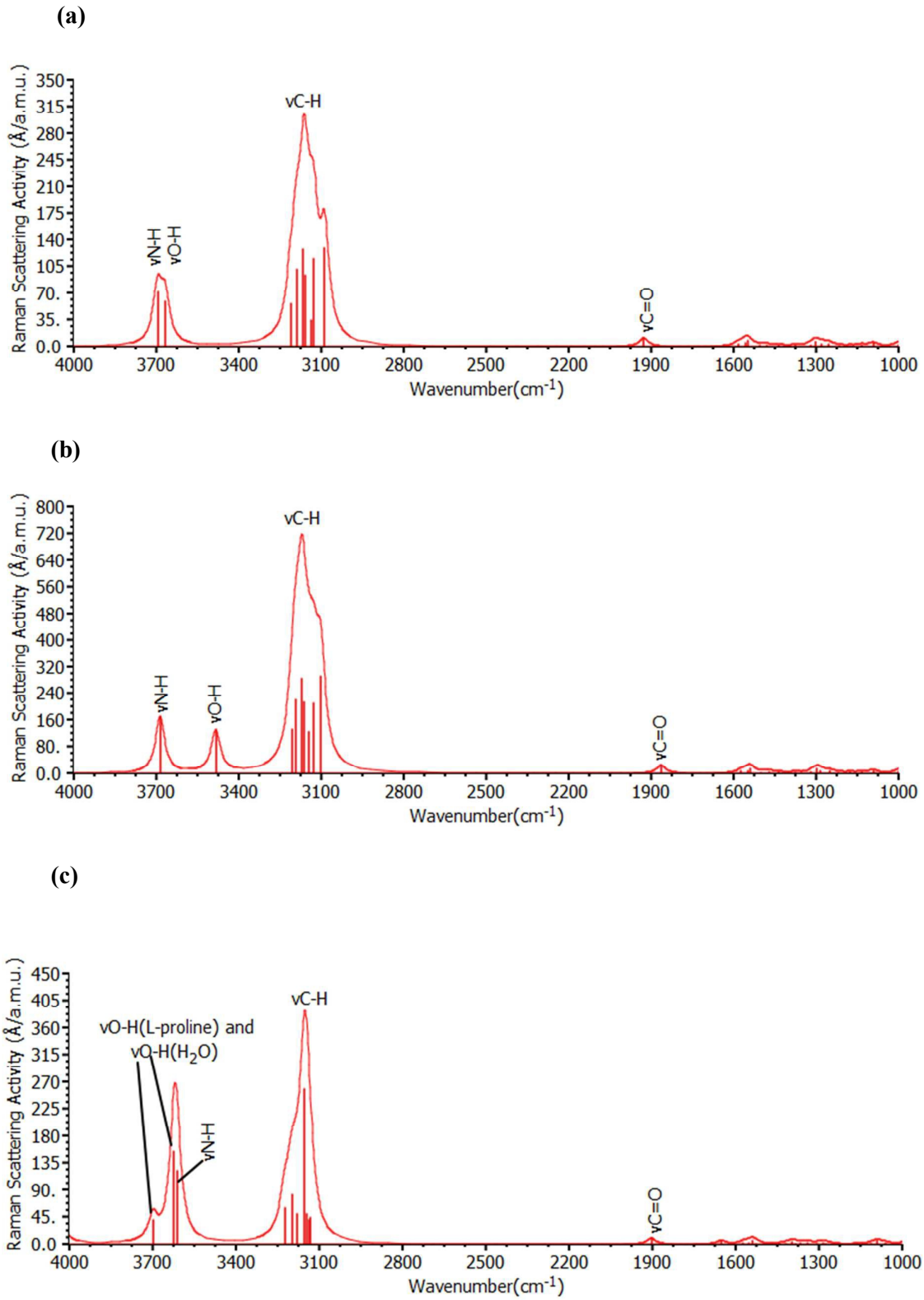

Figure 10. Computed Raman spectra of the conformer P1 of L-proline computed at the BHandHLYP/6-311++G(d,p) level of the theory: (a) isolated (gas-phase) P1, (b) P1 in water-solvent, (c) single-water molecule Complex 1a of conformer P1. The vertical lines, under the peaks, specify the location of the normal modes.

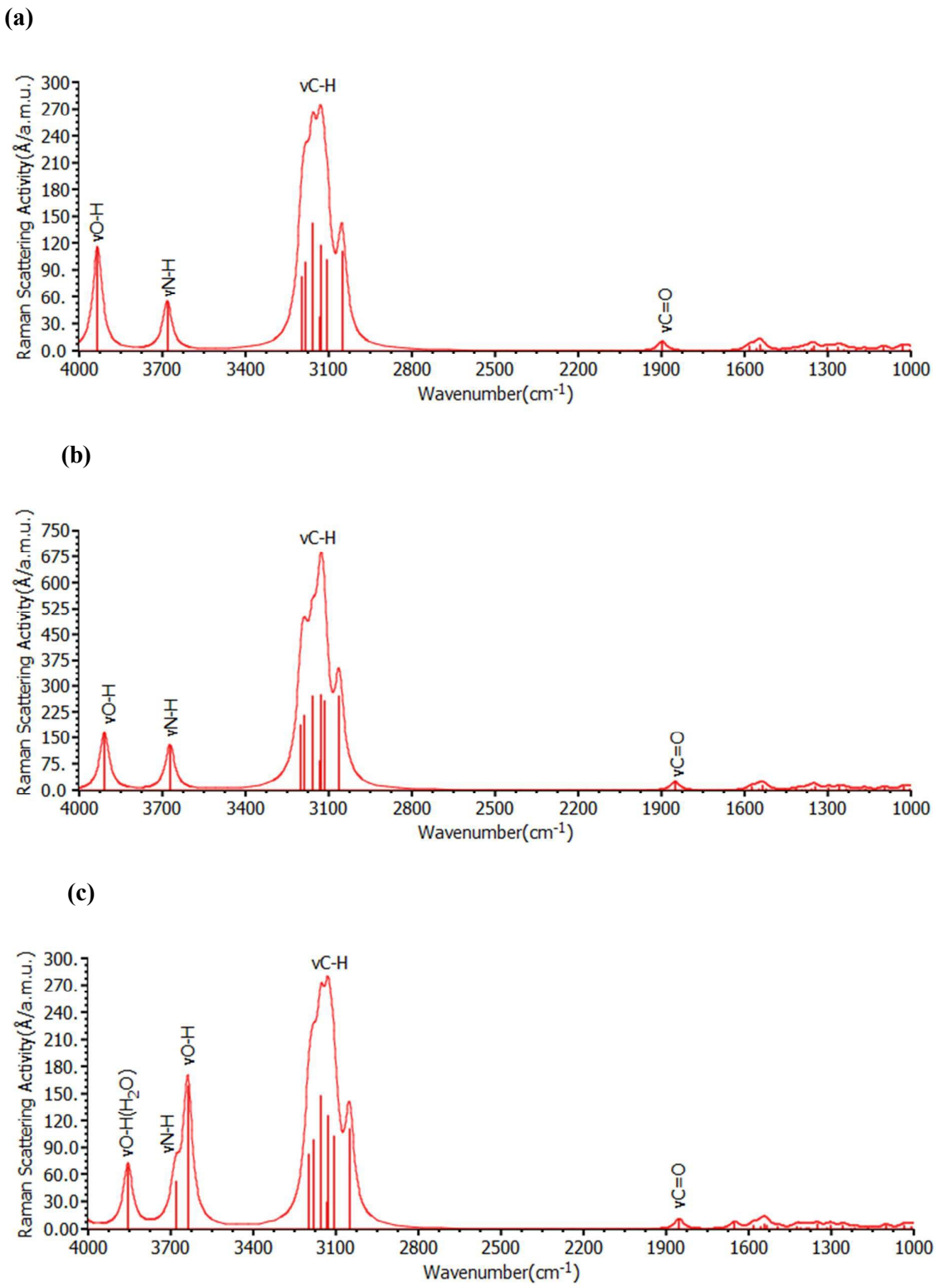

Figure 11. Same as Figure 10, but for the Raman spectra of conformer P4 of L-proline and its single-water molecule Complex 4b.

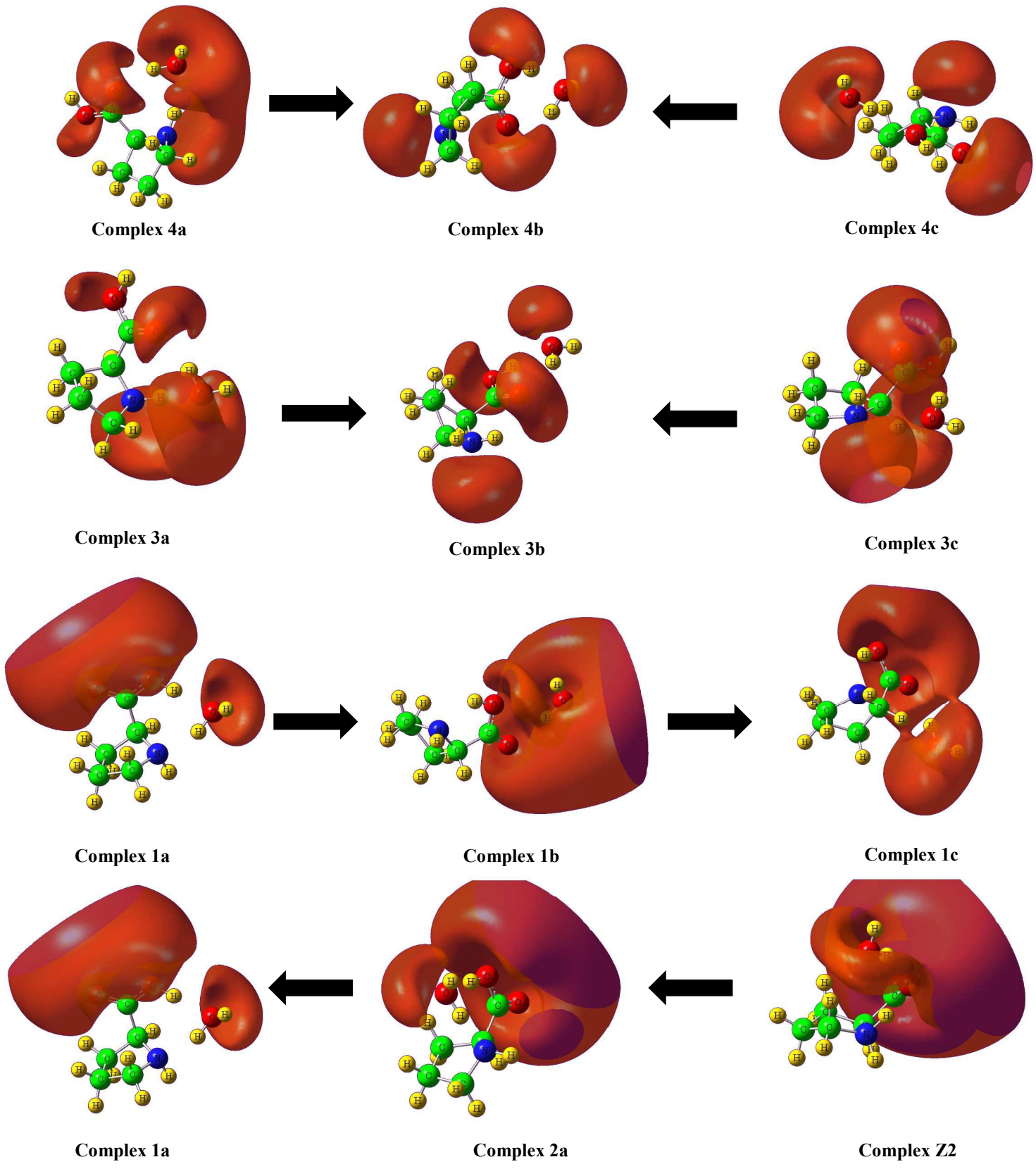

Figure 12. 3D surface (isovalue=0.02) of electrostatic potential (ESP) in the water-complexes of L-proline, corresponding to relevant water-migration pathways depicted in Figure 6: (a) from complex 4a → 4c, (b) from complex 3a → 3c, (c) from complex 1a → 1c, (d) from complex 1a → Z2. For simplicity, only the negative ESP is depicted. The direction of the arrow between the two complexes is towards more stable complex along the pathway.

Table 1. Standard Gibbs free energy change (ΔG) in kcal/mol, at the BHandHLYP/6-311++G(d,p) level of the theory, for the reaction pathways depicted in Figures 2, 3, 5 and supporting information Figure S4.

Reaction Pathways		ΔG (kcal/mol)	Reaction Pathways		ΔG (kcal/mol)
Figure 2			**Figure 5**		
Complex 1a	→ TS 1a/1b	-0.31	Complex 3a	→ TS 3a/3b	1.63
Complex TS 1a/1b	→ 1b	-4.39	Complex TS 3a/3b	→ 3b	-4.64
Complex 1b	→ TS 1b/1c	1.38	Complex 3b	→ TS 3b/3c	5.52
Complex TS 1b/1c	→ 1c	-0.94	Complex TS 3b/3c	→ 3c	-0.25
Complex 1c	→ TS 1c/1d	2.70	Complex 3a	→ TS 3a/3e	2.32
Complex TS 1c/1d	→ 1d	-1.13	Complex TS 3a/3e	→ 3e	-2.07
Complex 1d	→ TS 1a/1d	2.38	Complex 3e	→TS 3d/3e	43.67
Complex TS 1a/1d	→1a	0.31	Complex TS 3d/3e	→ 3d	-45.31
Complex 2b	→TS 2b/2c	0.88	Complex 4a	→ TS 4a/4b	0.88
Complex TS 2b/2c	→ 2c	-1.13	Complex TS 4a/4b	→ 4b	-4.08
Complex 1a	→ TS 1a/2a	1.44	Complex 4b	→ TS 4b/4c	4.96
Complex TS 1a/2a	→ 2a	-1.57	Complex TS 4b/4c	→ 4c	-0.94
Complex 1b	→ TS 1b/2b	2.64	Complex 4a	→ TS 4a/4d	64.95
Complex TS 1b/2b	→ 2b	-2.01	Complex TS 4a/4d	→ 4d	-66.27
Complex 1d	→ TS 1d/2d	2.26	Complex 3c	→TS 3c/4c	1.00
Complex TS 1d/2d	→ 2d	-1.76	Complex TS 3c/4c	→ 4c	-2.32
Figure 3			Complex 3d	→ TS 3d/4d	1.69
Complex 1a	→ TS 1a/Z1	12.86	Complex TS 3d/4d	→ 4d	-1.51
Complex TS 1a/Z1	→ Z1	-6.02	**Figure S4**		
Complex 2a	→ TS 2a/Z2	12.74	Complex 4a	→ TS 4a/4a	0.31
Complex TS 2a/Z2	→ Z2	-4.58	Complex 4b	→ TS 4b/4b	0.13

Table 2. Standard Gibbs free energy change (ΔG) in kcal/mol, relative to the separated species, at different temperatures, for the single-water molecule complexes of L-proline, at the BHandHLYP/6-311++G(d,p) level of the theory.

Complex	ΔG (kcal/mol)			
T (K)	100	200	298.15	400
1a	-0.13	-3.14	-6.09	-9.16
1b	2.70	0.31	-1.88	-9.16
1c	3.64	0.88	-1.76	-4.46
1d	1.76	-0.94	-3.45	-6.02
1e	2.07	-0.06	-1.95	-3.77
2a	0.63	-2.57	-5.71	-8.91
2b	2.89	0.63	-1.44	-3.51
2c	3.95	1.07	-1.76	-4.64
2d	1.57	-1.13	-3.77	-6.40
2e	2.20	0.13	-1.76	-3.58
3a	2.57	-0.38	-3.07	-5.90
3b	6.15	2.95	-0.06	-3.20
3c	0.31	-2.13	-4.39	-6.65
3d	3.70	1.00	-1.57	-4.27
3e	2.26	-0.50	-3.07	-5.71
4a	2.26	-14.68	-3.14	-5.90
4b	6.15	3.20	0.31	-2.76
4c	0.63	-1.69	-3.89	-6.09
4d	3.51	0.82	-1.82	-4.58

Table 3. Partial atomic charges on atoms, excluding H-atoms, in the zwitterionic and relevant neutral complexes of conformer P1 and P4 of L-proline with single-water molecule at BHandHLYP/6-311++G(d,p) level of the theory using Hirshfeld population analysis (HPA), charge-model 5 (CM5), Mülliken (MPA) and natural (NPA) population analysis. The values compared in parentheses correspond to partial atomic charges in the respective isolated conformers (without water).

Atom	**Complex Z1**				***Complex Z2***				**Complex 1a**				***Complex 4b***			
	HPA	**CM5**	**MPA**	**NPA**	***HPA***	***CM5***	***MPA***	***NPA***	**HPA**	**CM5**	**MPA**	**NPA**	***HPA***	***CM5***	***MPA***	***NPA***
								L-Proline								
N1	-0.01 (-0.18)	-0.53 (-0.55)	-0.08 (-0.32)	-0.61 (-0.74)	-0.01 (-0.18)	-0.52 (-0.55)	-0.11 (-0.27)	-0.60 (-0.74)	-0.17 (-0.18)	-0.54 (-0.55)	-0.28 (-0.32)	-0.72 (-0.74)	-0.21 (-0.21)	-0.57 (0.57)	-0.16 (-0.17)	-0.70 (-0.70)
C1	0.02 (0.00)	-0.04 (-0.06)	-0.35 (-0.30)	-0.15 (-0.15)	0.02 (0.00)	-0.04 (-0.06)	-0.48 (-0.35)	-0.17 (-0.16)	0.00 (0.00)	-0.06 (-0.06)	-0.37 (-0.30)	-0.17 (-0.15)	-0.01 (-0.01)	-0.06 (0.06)	-0.31 (-0.33)	-0.15 (-0.15)
C2	0.04 (0.03)	0.02 (0.02)	-0.25 (-0.10)	-0.10 (-0.11)	0.04 (0.03)	0.02 (0.02)	-0.16 (-0.19)	-0.09 (-0.11)	0.03 (0.03)	0.02 (0.02)	0.15 (-0.10)	-0.11 (-0.11)	0.03 (0.03)	0.03 (0.03)	-0.17 (-0.11)	-0.10 (-0.10)
C3	-0.05 (-0.06)	-0.15 (-0.16)	-0.41 (-0.42)	-0.39 (-0.39)	-0.05 (-0.06)	-0.16 (-0.16)	-0.23 (-0.24)	-0.38 (-0.38)	-0.06 (-0.06)	-0.17 (-0.16)	-0.30 (-0.42)	-0.40 (-0.39)	-0.06 (-0.06)	-0.16 (-0.16)	-0.38 (-0.37)	-0.38 (-0.38)
C4	-0.05 (-0.05)	-0.15 (-0.15)	-0.27 (-0.23)	-0.39 (-0.37)	-0.05 (-0.05)	-0.15 (-0.15)	-0.41 (-0.36)	-0.38 (-0.37)	-0.06 (-0.05)	-0.16 (-0.15)	-0.64 (-0.23)	-0.39 (-0.37)	-0.05 (-0.05)	-0.15 (-0.15)	-0.30 (-0.30)	-0.36 (-0.36)
C5	0.19 (0.24)	0.25 (0.29)	0.13 (0.00)	0.83 (0.85)	0.19 (0.24)	0.25 (0.29)	0.10 (0.04)	0.83 (0.85)	0.24 (0.24)	0.30 (0.29)	-0.05 (0.00)	0.85 (0.85)	0.26 (0.25)	0.31 (0.31)	0.02 (0.02)	0.88 (0.86)
O1	-0.36 (-0.22)	-0.44 (-0.41)	-0.47 (-0.17)	-0.85 (-0.71)	-0.35 (-0.22)	-0.43 (-0.41)	-0.47 (-0.17)	-0.85 (-0.71)	-0.22 (-0.22)	-0.42 (-0.41)	-0.30 (-0.17)	-0.72 (-0.71)	-0.30 (-0.31)	-0.36 (-0.37)	-0.36 (-0.33)	-0.70 (-0.64)
O2	-0.39 (-0.32)	-0.43 (-0.37)	-0.39 (-0.31)	-0.71 (-0.63)	-0.39 (-0.33)	-0.43 (-0.37)	-0.38 (-0.29)	-0.70 (-0.63)	-0.31 (-0.32)	-0.36 (-0.37)	-0.29 (-0.31)	-0.62 (-0.63)	-0.21 (-0.20)	-0.40 (-0.41)	-0.28 (-0.18)	-0.72 (-0.71)
								Water								
O3	-0.30	-0.68	-0.59	-0.97	-0.35	-0.68	-0.55	-0.96	-0.34	-0.65	-0.57	-0.97	-0.29	-0.64	-0.54	-0.96